

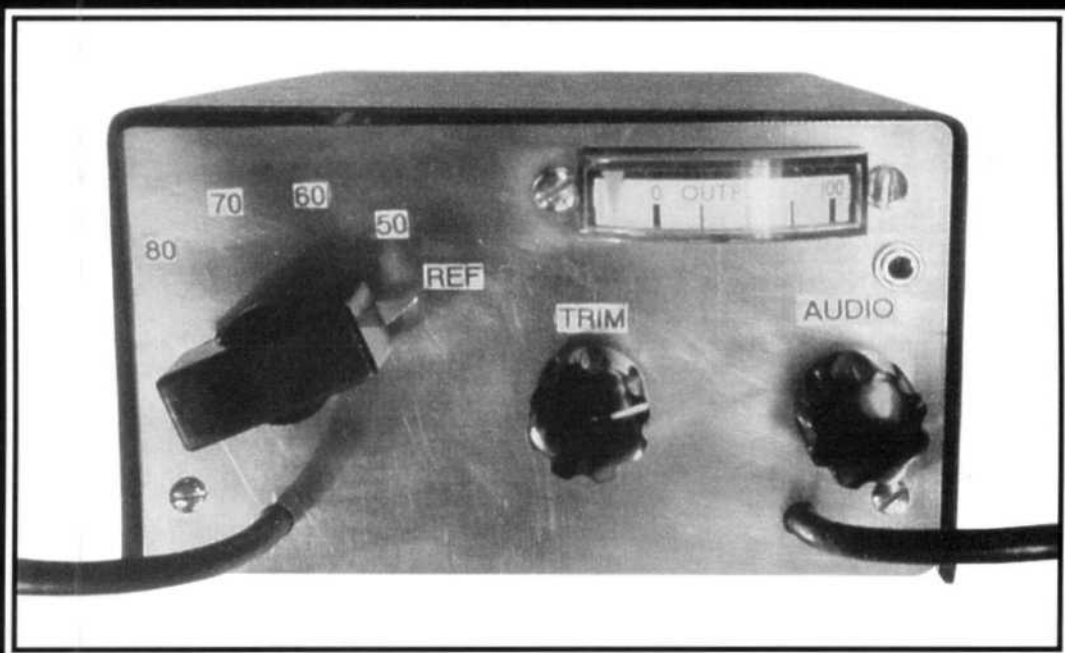
QEX

\$1.75



ARRL Experimenter's Exchange

July 1995



Spectral Analysis Without a Spectrum Analyzer

QEX: The ARRL
Experimenter's Exchange
American Radio Relay League
225 Main Street
Newington, CT USA 06111

QEX

QEX (ISSN: 0886-8093 USPS 011-424) is published monthly by the American Radio Relay League, Newington, CT USA.

Second-class postage paid at Hartford, Connecticut and additional mailing offices.

David Sumner, K1ZZ
Publisher

Jon Bloom, KE3Z
Editor

Lori Weinberg
Assistant Editor

Harold Price, NK6K
Zack Lau, KH6CP
Contributing Editors

Production Department

Mark J. Wilson, AA2Z
Publications Manager

Michelle Bloom, WB1ENT
Production Supervisor

Sue Fagan
Graphic Design Supervisor

Joe Costa
Technical Illustrator

Joe Shea
Production Assistant

Advertising Information Contact:

Brad Thomas, KC1EX, Advertising Manager
American Radio Relay League
203-667-2494 direct
203-666-1541 ARRL
203-665-7531 fax

Circulation Department

Debra Jahnke, Manager
Kathy Fay, N1GZO, Deputy Manager
Cathy Stepina, QEX Circulation

Offices

225 Main St, Newington, CT 06111-1494 USA
Telephone: 203-666-1541
Telex: 650215-5052 MCI
FAX: 203-665-7531 (24 hour direct line)
Electronic Mail: MCIMAILID: 215-5052
Internet: qex@arrl.org

Subscription rate for 12 issues:

In the US: ARRL Member \$12,
nonmember \$24;

US, Canada and Mexico by First Class Mail:
ARRL Member \$25, nonmember \$37;

Elsewhere by Surface Mail (4-8 week
delivery): ARRL Member \$20,
nonmember \$32;

Elsewhere by Airmail: ARRL Member \$48,
nonmember \$60.

QEX subscription orders, changes of address, and reports of missing or damaged copies may be marked: QEX Circulation. Postmaster: Form 3579 requested. Send change of address to: American Radio Relay League, 225 Main St, Newington, CT 06111-1494.

Members are asked to include their membership control number or a label from their QST wrapper when applying.

Copyright © 1995 by the American Radio Relay League Inc. Material may be excerpted from QEX without prior permission provided that the original contributor is credited, and QEX is identified as the source.



About the Cover

No spectrum analyzer handy? As W6IOJ shows, you can make spectral measurements with simpler, home-built equipment.

ISSUE
NO.
161



Features

3 The Effect of Local Terrain on HF Launch Angles

By R. Dean Straw, N6BV

16 Spectral Measurements the Hard Way

By John C. Reed, W6IOJ

21 A Termination Insensitive Amplifier

By Jacob Makhinson, N6NWP

Columns

29 Upcoming Technical Conferences

July 1995 QEX Advertising Index

American Radio Relay League: 30,
Cov IV
Communications Specialists Inc: 31
Down East Microwave Inc: 30
LUCAS Radio/Kangaroo Tabor
Software: 31

PacComm: Cov II, Cov III
PC Electronics: 30
Tucson Amateur Packet Radio Corp: 32
Z Domain Technologies, Inc: 31

THE AMERICAN RADIO RELAY LEAGUE



The American Radio Relay League, Inc. is a noncommercial association of radio amateurs, organized for the promotion of interests in Amateur Radio communication and experimentation, for the establishment of networks to provide communications in the event of disasters or other emergencies, for the advancement of radio art and of the public welfare, for the representation of the radio amateur in legislative matters, and for the maintenance of fraternalism and a high standard of conduct.

ARRL is an incorporated association without capital stock chartered under the laws of the state of Connecticut, and is an exempt organization under Section 501(c)(3) of the Internal Revenue Code of 1986. Its affairs are governed by a Board of Directors, whose voting members are elected every two years by the general membership. The officers are elected or appointed by the Directors. The League is noncommercial, and no one who could gain financially from the shaping of its affairs is eligible for membership on its Board.

"Of, by, and for the radio amateur," ARRL numbers within its ranks the vast majority of active amateurs in the nation and has a proud history of achievement as the standard-bearer in amateur affairs.

A bona fide interest in Amateur Radio is the only essential qualification of membership; an Amateur Radio license is not a prerequisite, although full voting membership is granted only to licensed amateurs in the US.

Membership inquiries and general correspondence should be addressed to the administrative headquarters at 225 Main Street, Newington, CT 06111 USA.

Telephone: 203-666-1541
Telex: 650215-5052 MCI
MCIMAIL (electronic mail system) ID: 215-5052
FAX: 203-665-7531 (24-hour direct line)

Officers

President: GEORGE S. WILSON III, W4OYI
1649 Griffith Ave, Owensboro, KY 42301

Executive Vice President: DAVID SUMNER, K1ZZ

Purpose of QEX:

- 1) provide a medium for the exchange of ideas and information between Amateur Radio experimenters
- 2) document advanced technical work in the Amateur Radio field
- 3) support efforts to advance the state of the Amateur Radio art

All correspondence concerning QEX should be addressed to the American Radio Relay League, 225 Main Street, Newington, CT 06111 USA. Envelopes containing manuscripts and correspondence for publication in QEX should be marked: Editor, QEX.

Both theoretical and practical technical articles are welcomed. Manuscripts should be typed and doubled spaced. Please use the standard ARRL abbreviations found in recent editions of *The ARRL Handbook*. Photos should be glossy, black and white positive prints of good definition and contrast, and should be the same size or larger than the size that is to appear in QEX.

Any opinions expressed in QEX are those of the authors, not necessarily those of the editor or the League. While we attempt to ensure that all articles are technically valid, authors are expected to defend their own material. Products mentioned in the text are included for your information; no endorsement is implied. The information is believed to be correct, but readers are cautioned to verify availability of the product before sending money to the vendor.

Empirically Speaking

Summertime and the Living is...Hot!

Experimenters always seem to have more project ideas in mind than there is time to do them. There's always a new, exciting project to get working on. But hey, it's too hot to be slaving over a hot soldering iron, so how about doing a little maintenance of the existing electronic and antenna systems? Here at ARRL HQ, the mid-June preparations for Field Day included some general maintenance of the satellite antenna system atop the HQ building.

Boy, are we glad we worked on the system! Over the past few years the performance had degraded and we weren't even aware of it! Suddenly, after fixing all of the little problems and cleaning and tightening the connections, system performance is back to its peak of a few years ago.

Of course, we shouldn't really need a reminder that regular maintenance of electronic and mechanical systems is needed to keep them in top shape, but when it's a struggle to find time for the new projects, maintaining the completed projects tends to slip.

Take our advice: set aside a day or two to do some maintenance. Clean the air filters on blower-equipped units. Tighten RF connectors to the correct torque. Check the waterproofing on external connectors and boxes. Replace corroded antenna hardware and tighten loose bolts. Check the loss of that 10-year-old feed line.

Yeah, it's hot outside. So get the outside work done before it turns cold!

KH6CP/1 Shall Return

Due to space constraints, Zack Lau's "RF" column does not appear this month. Never fear, though, Zack will return with his unique

brand of RF hints, helps and ideas in future issues.

The Incredible Lateness of QEX

You'll have noticed, no doubt, that you received this July issue of QEX in August, or nearly so. There's a reason for that, and his name is Robert Jonathan Bloom, who was born on July 7, 1995 (two weeks late, but loudly healthy). Now that he's here, we anticipate getting QEX back onto its normal production schedule; future issues should arrive on time!

This Month in QEX

Computer modeling of the performance of HF antenna systems has become a standard part of the serious HF amateur's station design. Problem is, the presently available tools make some unrealistically simplifying assumptions about the ground over which the antenna is operating. Since few of us operate our stations in free space or over flat ground, we need to model "The Effect of Local Terrain on HF Launch Angles," and that's what R. Dean Straw, N6BV, has done with his YPAD software.

If you don't have a spectrum analyzer handy to test that new home-built transmitter design, how can you be sure it's clean? By making "Spectral Measurements the Hard Way," at each discrete spurious frequency. But the hard way is made easier by the measurement system that John C. Reed, W6IOJ, describes.

A complex load such as a crystal filter can create havoc with a post-mixer amplifier, and if that amplifier passes the load variations to the mixer output, you won't likely get the mixer performance you want. One way of addressing this problem is use of "A Termination Insensitive Amplifier," by Jacob Makhinson, N6NWP.—KE3Z, email: jrbloom@arrl.org (Internet)

The Effect of Local Terrain on HF Launch Angles

*Introducing the YTAD Program —
Yagi Terrain Analysis, with Diffraction*

By R. Dean Straw, N6BV

Introduction

I'll admit it—my first love in Amateur Radio is HF contesting. I operate in short, but very intense, bursts of activity (usually 48 hours long), concentrated during the months of October, November, February and March. True contest junkies recognize these as the months for the major DX contests, and for the ARRL Sweepstakes too. During the rest of the year, I can usually be found scheming and dreaming about what I must do to improve the station for next year's contests.

This article describes a work-in-progress, focusing on how local terrain affects the propagation of signals for DX work. I will describe an experimental IBM-PC computer program de-

signed to analyze the effects of local terrain. The advantages, pitfalls and perils of its use are laid out. I will also ask for help in validating the results from you, the readers.

Contest QTHs

The last major study that appeared in the amateur literature on the subject of local terrain as it affects DX appeared in four *QST* "How's DX?" columns, by Clarke Green, K1JX, from October 1980 to January 1981. Greene's work was an update of a landmark September 1966 *QST* article entitled "Station Design for DX," by Paul Rockwell, W3AFM. I highly recommend that you reread both Greene's and Rockwell's articles. I was particularly fascinated by the long-range profiles of several prominent, indeed legendary, stations in Rockwell's article: W3CRA, W4KFC and W6AM.

The subject of how to choose a QTH

for working DX has fascinated hams since the beginning of amateur operations. Marconi probably spent a lot of time wandering around Newfoundland looking for a great radio QTH. I'm sure you've all heard someone at your local club drooling over a location he wanted to buy, one that just "smelled of DX."

Putting together a high-performance HF station for contesting or DXing has always followed some pretty simple rules. First, and most obvious, you need the perfect QTH, preferably on a rural mountain top or at least on top of a hill. Even better yet, you need a mountain top surrounded by seawater! Some of the contesters around HQ fondly reminisce about the famous "Residence," a swamp on a hill, where K1ZZ and company held forth for a number of years with their fabled rock-crusher 80-meter signal.

Then, after you have found your

dream QTH, you put up the biggest antennas you possibly can, on the highest, strongest towers you can afford. Then you work all sorts of DX—sunspots willing, of course.

The only trouble with this straightforward formula for success is that it doesn't always work. Hams fortunate enough to be located on mountain tops with really spectacular drop-offs often find that their highest antennas don't do very well, especially on 15 or 20 meters, but often even on 20 meters. When they compare their signals with nearby locals in the flatlands, they sometimes (but not always) come out on the short end of the stick, especially when sunspot activity is high.

On the other hand, when the sunspots drop into the cellar, the high antennas on the mountain top are usually the ones crunching the pile-ups—but again, not always. So, the really ambitious contest aficionados, the guys with lots of resources and infinite enthusiasm, have resorted to putting up antennas at all possible heights, on a multitude of towers. At one time, super contester N5AU had something like 17 towers in the air, with lots and lots of aluminum all over them. A respectable multi-multi station nowadays usually has at least five towers, often substantially more.

Maybe it's me, but perhaps you too have noticed that the operating consoles at the super stations that make the front cover of *CQ* look like the owners have stock in companies that make coax switches. It stands to reason—one antenna out of a whole bunch of them was bound to be a winner on any particular band, so put up lots and lots of antennas and select them using lots and lots of coax switches!

Clearly, there has to be a more scientific way to figure out where and how high to put your antennas to optimize your signal during all parts of the 11-year solar cycle. In this article, I will advocate a *system approach* to HF station design, in which you need to know the following:

1. the range of elevation angles necessary to get from point A to point B;
2. the elevation patterns for various types and configurations of antennas; and
3. the effect of local terrain on antenna elevation patterns.

What Is the Range of Elevation Angles Needed?

Until 1994, *The ARRL Antenna*

Book contained only a limited amount of information concerning the elevation angles needed for communication throughout the world. In the 1974 edition, Table 1-1 in the Wave Propagation chapter was captioned: "Measured vertical angles of arrival of signals from England at receiving location in New Jersey."

What the caption didn't say was that Table 1-1 was derived from measurements made during 1934 by Bell Labs. To me, the highest frequency data seemed pretty shaky, considering that 1934 was the low point of Cycle 17. Neither was this data applicable to any path other than the one from New Jersey to England. Nonetheless, many amateurs located throughout the US (and I suspect throughout the world too) tried to use the sparse information in Table 1-1 as the only rational data they had for determining how high to mount their antennas. (If they lived on hills, they made estimates of the effect of the terrain, assuming that the hill was adequately represented by a long, unbroken slope. More on this later.)

One of the first tasks I was given when I joined ARRL HQ was to tabulate the range of elevation angles from all regions of the US to important DX QTHs around the world. This was accomplished by running many thousands of computations using the *IONCAP* computer program. *IONCAP*

has been under development for more than 25 years by various agencies of the US government and is considered the standard of comparison for propagation programs by many agencies, including the Voice of America, Radio Free Europe, and more than 100 foreign governments throughout the world. *IONCAP* is a real pain in the neck to use, but it *is* the standard of comparison.

My calculations were done for all levels of solar activity, for all months of the year, and for all 24 hours of the day. I gathered the results into some very large databases and extracted detailed statistics from these. The results appear in summary form in Tables 4 through 13 printed in the "Radio Wave Propagation" chapter of the 17th edition of *The ARRL Antenna Book*.

Fig 1 reproduces Fig 28 from the 17th edition of *The ARRL Antenna Book*. This depicts the full range of elevation angles for the 20-meter path from Newington, CT, to all of Europe. This is for all openings, in all months, over the entire 11-year solar cycle. The most likely elevation angle occurs between 10° to 12° for about 46% of the times when the band is open. There is a secondary peak between 4° to 6°, occurring for about 29% of the time the band is open.

In Fig 1, the statistical angle infor-

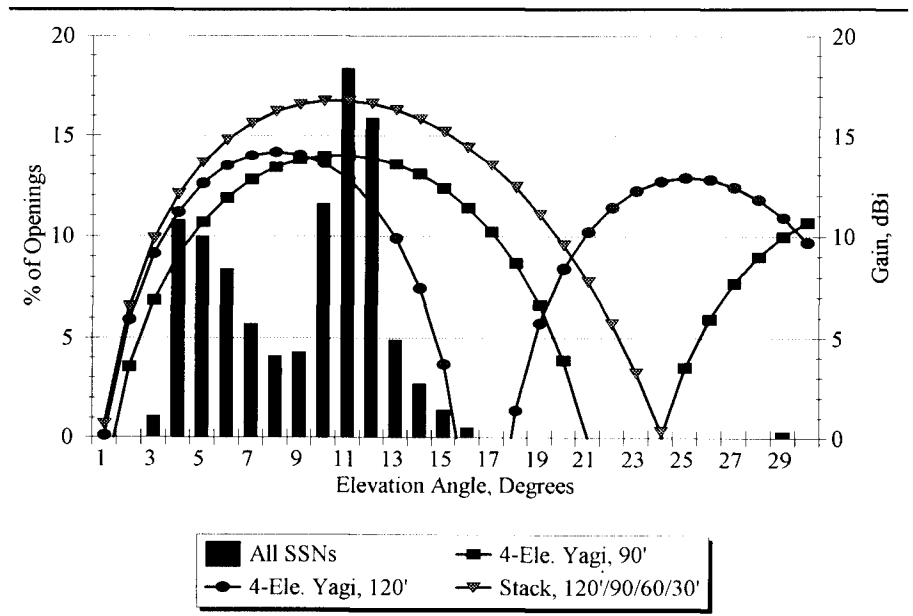


Fig 1—Graph showing percentage of all 20-meter openings from New England to Europe versus elevation angles, together with overlay of elevation patterns over flat ground for three 20-meter antenna systems. The most statistically likely angle at which the band will be open is 11°, although at any particular hour, day, month and year, the actual angle may well be different.

mation is also overlaid with the elevation responses for three different antenna configurations, all mounted over flat ground. The stack of four 4-element Yagis at 120, 90, 60 and 30 feet best covers the whole range of necessary elevation angles among the three systems shown, with the best single antenna arguably being the 90-foot high Yagi.

There was insufficient room in *The ARRL Antenna Book* to print out reams and reams of really detailed information computed for each US callsign location, so the detailed data is located in the \ELEVAT subdirectory on the diskette bundled with the 17th edition. You will find there 60 *.PRN files in ASCII format, each about the size of a full sheet of paper when printed out. Each contains detailed statistical information on elevation angles for all the HF ham bands, from all ten US call districts (W1 to W0) to six geographic areas throughout the world: Europe, South America, the Far East, Southern Asia, Southern Africa and the South Pacific.

Now, I must emphasize that these are *statistical entities*—in other words, just because 11° is the “statistically most likely angle” for the 20-meter path from New England to Europe doesn’t mean that the band will be open at 11° at any particular hour, on a particular day, in a particular month, in any particular year! In fact, experience agrees with the *IONCAP* computations: the 20-meter path to Europe from New England usually opens at a low angle in the morning hours, rising to about 11° during the afternoon, when the signals remain strongest throughout the afternoon until the evening.

Now see Fig 2. Just because 5° is the statistically most prevalent angle (occurring some 21% of the time) from Seattle to Europe on 20 meters, this doesn’t mean that the actual angle *at any particular moment in time* might not be 10°, or even 2°. The statistics for W7 to Europe say that 5° is the most likely angle, but 20-meter signals from Europe arrive at angles ranging from 1° to 12°. If you design an antenna system to cover all possible angles needed to talk to Europe from Seattle on 20 meters, you would need to cover the full range from 1° to 12° equally well.

Similarly, if you wish to cover the full range of elevation angles from Chicago to Southern Africa on 15° meters, you would need to cover 1° to 14°, even though the most statistically likely signals arrive at 10°, for 34% of

the time when that the band is open for that path. See Fig 3.

It takes a bit of careful study, but US radio amateurs have access to a great deal of statistical elevation-angle data in the 17th edition of *The ARRL Antenna Book*. Determining what

angles you must cover is the first part of a true *system design* for HF.

Drawbacks of Computer Models for Antennas Over Real Terrain

Modern general-purpose antenna modeling programs such as *NEC*¹ or

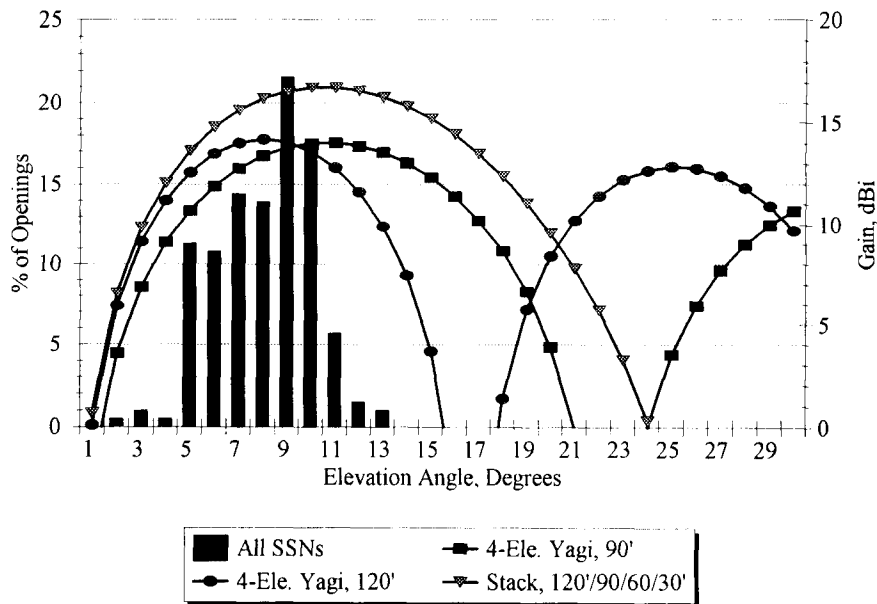


Fig 2—Graph showing percentage of all 20-meter openings, this time from Seattle, WA, to Europe, together with overlay of elevation patterns over flat ground for three 20-meter antenna systems. The statistically most likely angle on this path is 9°, occurring about 22% of the time when the band is actually open. Higher antennas predominate on this path.

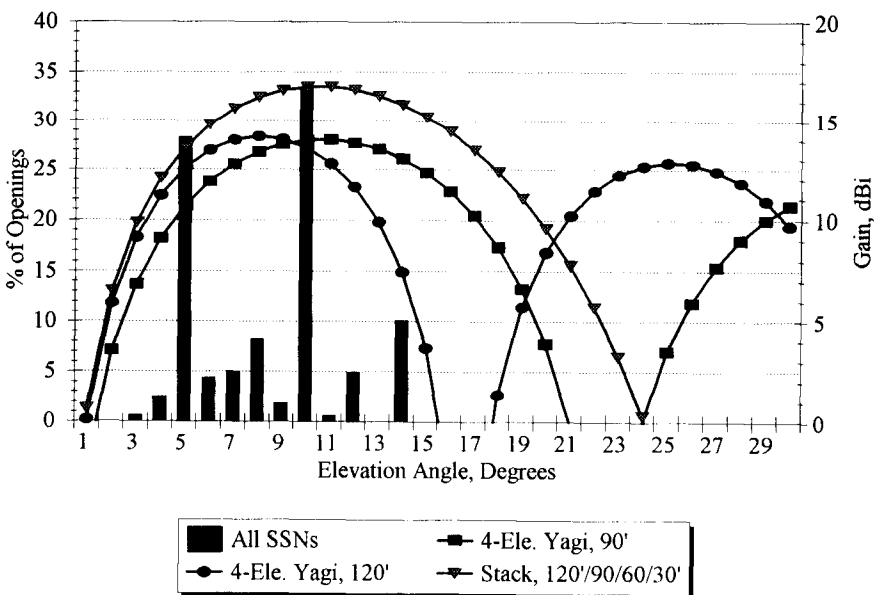


Fig 3—Graph showing percentage of all 20-meter openings from Chicago to Southern Africa, together with overlay of elevation patterns over flat ground for three 20-meter antenna systems. On this long-distance path, higher antennas are most effective.

*MININEC*² (or their commercially upgraded equivalents, such as *NEC/Wires*³ or *EZNEC*⁴) can accurately model almost any type of antenna commonly used by radio amateurs. In addition, there are specialized programs specifically designed to model Yagis efficiently, such as *YO*⁵ or *YagiMax*.⁶

I will not attempt to describe the wide range of antenna-modeling software available to the ham, since that subject has already been well covered in a number of other arenas. However, I will discuss one aspect important in this article—the ability/inability to model antennas over anything other than *purely flat ground*.

Programs such as *NEC* are wonderful for modeling antennas in free space. They can also do a great job modeling antennas over flat ground. They can even model antennas electrically very close to the ground, such as wires only inches off flat ground. However, these programs have real limitations when it comes to real terrain. While both *NEC* and *MININEC* can simulate irregular ground terrain, they do so in a decidedly crude manner, employing step-like concentric rings of height around an antenna. The documentation for *NEC* and *MININEC* both clearly state that diffraction off these “steps” is not modeled. Common experience among serious modelers is that the warnings in the manuals are well worth heeding!

Although analysis and even optimization of antenna designs can be done using free-space or flat-earth ground models, it is *diffraction* that makes the real world a very, very complicated place indeed. I should clarify this—diffraction is hard, even tortuous, to analyze properly, but it makes analysis of real-world results far more believable than a flat-world reflection model does.

Ray-Tracing the Effect of Local Terrain on Antenna Elevation Patterns

My First Attempts— Some Tantalizing Clues

Several years ago, Bill Myers, K1GQ, provided me with some crucial insights into the methodology for terrain modeling. He shared with me a *MathCAD* type of model using ray-tracing and perfect reflection off the terrain ahead of the antenna. In essence, from a specified height on the

tower, an antenna would shoot “rays” (just like bullets) in quarter-degree increments from +35° above the horizon to -35° below the horizon. Each ray is traced over the foreground terrain to see if it hits the ground at any point on its travels in the direction of interest. If it does hit the ground, the ray is reflected following the classical “law of reflection.” That is, the outgoing angle equals the incoming angle, reflected through the normal to the slope of the surface. Once the rays exit into the ionosphere, the individual contributions are vector-summed to create the overall far-field elevation pattern.

One of my first attempts at modeling the effects of foreground terrain was called *RTF*, standing for “Ray-Tracing with Fresnel.” (Catchy name, don’t you think?) *RTF* used K1GQ’s simple ray-tracing algorithm for reflections. I added in complex horizontally polarized Fresnel ground coefficients, using the formulas described by Charlie Michaels, W7XC, in *The ARRL Antenna Compendium, Vol 3*.⁷

My *RTF* program was written in *QuickBASIC*. It took me to the outer edges of BASIC’s capabilities since I was trying to handle huge matrices of complex variables. (By the way, I should note that K1GQ was correct when he told me that the addition of the Fresnel ground coefficients wouldn’t greatly alter the results, since I was only considering horizontally polarized antennas.)

Despite the simplicity of the model, *RTF* gave a lot of insights into the effects of foreground terrain. However, it always seemed to give gain figures that were optimistic, particularly at very low elevation angles. Something was definitely missing from this classical ray-tracing model using only reflection techniques, even with the Fresnel ground coefficients added in for good measure.

At the Dayton antenna forum in 1994, Jim Breakall, WA3FET, gave a fascinating and tantalizing lecture on the effect of foreground terrain. Later Breakall, Dick Adler, K3CXZ, Joel Young and a group of other researchers published an extremely interesting paper entitled “The Modeling and Measurement of HF Antenna Skywave Radiation Patterns in Irregular Terrain” in the July 1994 *IEEE Transactions on Antennas and Propagation*.⁸ They described in rather general terms the modifications they made to the *NEC-BSC* program. They showed how the addition of a ray

tracing reflection and diffraction model to the simplistic stair-stepped reflection model in regular *NEC* gave far more realistic results. They compared actual pattern measurements made on a site in Utah (with an overflying helicopter) to computed patterns made using the modified *NEC* software. This sounded like great stuff—I desperately wanted the program! However, because the work was funded by the US Navy, the software was, and still is, a military secret.

Nevertheless, their paper eloquently made the case that diffraction effects were essential for evaluation of skywave elevation patterns resulting from the interaction of real-world antennas with real-world terrains. While Jim Breakall was constrained from providing actual software, he was nevertheless very kind and pointed me in the right direction to find relevant technical literature.

After studying the literature, I realized that the techniques employed in *RTF* were using primitive “Geometric Optics.” If I wanted to get with the program, so to speak, I had to dive headlong into the really wild and woolly world of the “Uniform Theory of Geometric Diffraction.” In the many months I spent trying to figure out these often frustrating abstractions, my wife began to call my obsession the “Uniform Theory of *Distraction*.” She was right.

Brief History of The Uniform Theory of Diffraction

It is instructive to look briefly at the history of how “Geometric Optics” (GO) evolved (and still continues to evolve) into the “Uniform Theory of Diffraction” (UTD). The following is summarized from the historical overview in one book I found to be particularly useful and comprehensive on the subject of UTD: *Introduction to the Uniform Geometrical Theory of Diffraction*, by McNamara, Pistorius, and Malherbe.⁹

Many years before the time of Christ, the ancient Greeks studied optics. Euclid is credited with deriving the law of reflection about 300 BC and other Greeks, such as Ptolemy, were also fascinated with optical phenomena.

In the 1600s, a Dutchman named Snell finally figured out the law of refraction, resulting in *Snell’s law*. By the early 1800s, the basic world of classical optics was pretty well fleshed out from a mathematic point of view, based on the work of a number of individuals.

¹Notes appear on page 15.

As its name implies, classical geometric optical theory deals strictly with geometric shapes. Of course, the importance of geometry in optics shouldn't be minimized; otherwise many of us would have a tough time focusing on articles like this—we wouldn't have eyeglasses without geometric optics!

Mathematical analysis of shapes utilizes a methodology that traces the paths of straight-line rays of light. (Note that the paths of rays can also be likened to the straight-line paths of particles.) In classical geometric optics, however, there is no mention of three important quantities: phase, intensity and polarization. Indeed, without phase, intensity or polarization, there is no way to deal properly with the phenomenon of *interference*, or its cousin, *diffraction*. These phenomena require theories that deal with *waves* rather than rays.

Wave theory has also been around for a long time, although not as long as geometry. Workers like Hooke and Grimaldi recorded their observations of interference and diffraction in the mid 1600s. Huygens used elements of wave theory in the late 1600s to help explain refraction. By the late 1800s, the work of Lord Rayleigh, Sommerfeld, Fresnel, Maxwell and many others led to the full mathematic characterization of all electromagnetic phenomena, light included.

The mathematic elegance of wave theory is indisputable. Still, it's pretty safe to say that most people have a *lot* more trouble relating viscerally to a partial differential equation than they do to the concept of shooting a bullet at a target and watching the resulting ricochets! Shooting a "ray" at a target and predicting reflections, refractions and diffractions is somehow very satisfying and understandable at the gut-level. Unfortunately, ray-theory doesn't work for many problems, at least ray-theory in the classical optical form.

Now let's be fair—while wave theory is mathematically "universal," practical applications are few and far between. Mathematicians state that the "boundary conditions" for most physical situations are not exact. In other words, the real world is a lot more jagged, pointy and fuzzy in shape than can be described in a totally rigorous mathematic fashion.

To get a handle on a typical real-world physical situation, a combination of classical ray theory and wave theory was needed. Now doesn't this

bring back to mind our high-school physics classes where the "duality of particles and waves" was explained? Some properties of the real world are most easily explained on the micro level using electrons and protons as conceptual objects, while other macro phenomena (like resonance, for example) are more easily explained in terms of waves.

The breakthrough in the combination of classical geometric optics and wave concepts came from J. B. Keller of Bell Labs in 1953, although he published his work in the early 1960s.¹⁰ In the very simplest of terms, Keller introduced the notion that shooting a ray at a diffraction "wedge" causes wave interference at the tip, with an infinite number of diffracted waves emanating from the diffraction point. Each diffracted wave can be considered to be a point source radiator at the place of generation, the diffraction point. Thereafter, the paths of individual waves can be traced as though they were individual classical optic rays again. What Keller came up with was a reasonable mathematical description of what happens at the tip of the diffraction wedge.

Fig 4 is a picture of a simple diffraction wedge, with an incoming ray launched at an angle of α_r , referenced to the horizon, impinging on it. The diffraction wedge here is considered to be perfectly conducting, and hence impenetrable by the ray. The wedge generates an infinite number of

diffracted waves, going in all directions not blocked by the wedge itself. The amplitudes and phases of the diffracted waves are determined by the interaction at the wedge tip, and this in turn is governed by the various angles associated with the wedge. Shown in Fig 4 are the included angle α of the wedge, the angle ϕ' of the incoming ray (referenced to the incoming surface of the wedge), and the observed angle ϕ of one of the outgoing diffracted waves, also referenced to the wedge surface.

The so-called "shadow boundaries" are also shown in Fig 4. The Reflection-Shadow Boundary (RSB) is the angle beyond which no further reflections can take place for a given incoming angle. The Incident-Shadow Boundary (ISB) is that angle beyond which the wedge's face blocks any incident rays from illuminating the observation point.

Keller derived the amplitude and phase terms by comparing the classical Geometric Optics (GO) solution with the exact mathematical solution calculated by Sommerfeld for a particular case where the boundary conditions were well known—an infinitely long, perfectly conducting wedge illuminated by a plane wave. Simply speaking, whatever was left over had to be diffraction terms. Keller combined these diffraction terms with GO terms to yield the total field everywhere.

Keller's new theory became known as the Geometric Theory of Diffraction

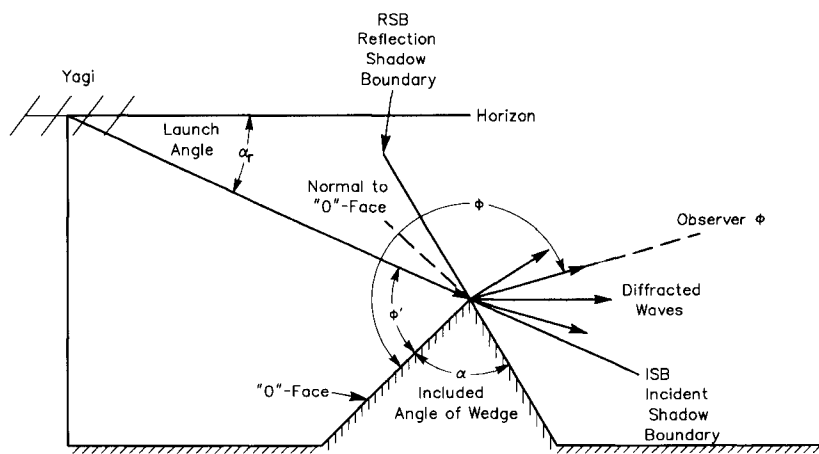


Fig 4—Diagram showing diffraction mechanism of ray launched at angle α_r below horizon at diffraction wedge, whose included angle is α . Referenced to the incident face (the "o-face" as it is called in UTD terminology), the incoming angle is ϕ' . The wedge creates an infinite number of diffracted waves. Shown is one whose angle referenced to the o-face is ϕ , the so-called "observation angle" in UTD terminology.

(abbreviated henceforth as GTD). The beauty of GTD was that in the regions where classical GO predicted zero fields, the GTD “filled in the blanks,” so to speak. For example, see Fig 5, showing the terrain for a hypothetical case, where a 60-foot high 4-element 15-meter Yagi illuminates a wide, perfectly flat piece of ground. A 10-foot high rock has been placed 400 feet away from the tower base in the direction of outgoing rays. Fig 6 shows the elevation pattern predicted using reflection-only GO techniques. Due to blockage of the direct wave (A) trying to shoot past the 10-foot high rock, and due to blockage of (B) reflections from the flat ground in front of the rock by the rock, there is a “hole” in the smooth elevation pattern.

Now, doesn't it defy common sense to imagine that a single 10-foot high rock will really have such an effect on a 15-meter signal? Keller's GTD took diffraction effects into account to show that waves do indeed sneak past and over the rock to fill in the pattern. The whole GTD scheme is very clever indeed.

However, GTD wasn't perfect. Keller's GTD predicts some big spikes in the pattern, even though the overall shape of the elevation pattern is much closer to reality than a simple GO reflection analysis would indicate. The region right at the RSB and ISB shadow boundaries is where problems are found. The GO terms go to zero at these points because of blockage by the wedge, while Keller's diffraction terms tend to go to infinity at these very spots. In mathematical terms this is referred to as a “caustic problem.” Nevertheless, despite these nasty problems at the ISB and RSB, the GTD provided a remarkably better solution to diffraction problems than did classical GO.

In the early 1970s, a group at Ohio State University under R. G. Kouyoumjian and P. H. Pathak did some pivotal work to resolve this caustic problem, introducing what amounts to a clever “fudge factor” to compensate for the tendency of the diffraction terms at the shadow boundaries to go to infinity.¹¹ They introduced what is known as a “transition function,” using a form of Fresnel integral. Most importantly, the Ohio State researchers also created several FORTRAN computer programs to compute the amplitude and phase of diffraction components. Now we computer hackers could get to work!

In the years since, other researchers have carried on extensive work in the

field of UTD. Not an issue of *The IEEE Transactions on Antennas and Propagation* goes by without at least an article or two about special, applied

aspects of the UTD. Most of them are written in dense, hyper-technical language that most hams have a very hard time relating to, myself included!

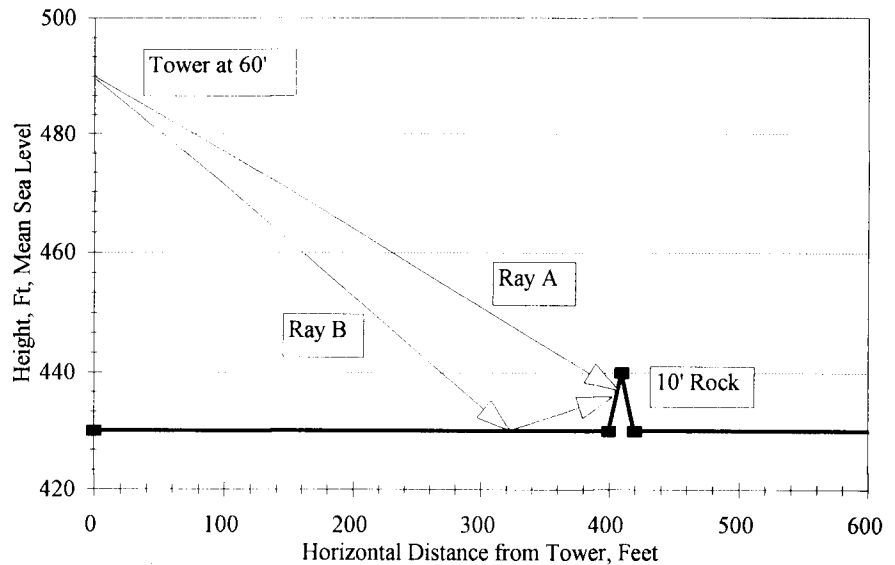


Fig 5—Hypothetical terrain exhibiting so-called “10-foot rock effect.” The terrain is flat from the tower base out to 400 feet, where a 10-foot-high rock is placed. Note that this forms a diffraction wedge but that it also blocks direct waves trying to shoot through it to the flat surface beyond, as shown by Ray A. Ray B reflects off the flat surface before it reaches the 10-foot rock but is blocked by the rock from proceeding further. A simple Geometric Optics (GO) analysis of this terrain without taking diffraction into account will result in the elevation response shown in Fig 6.

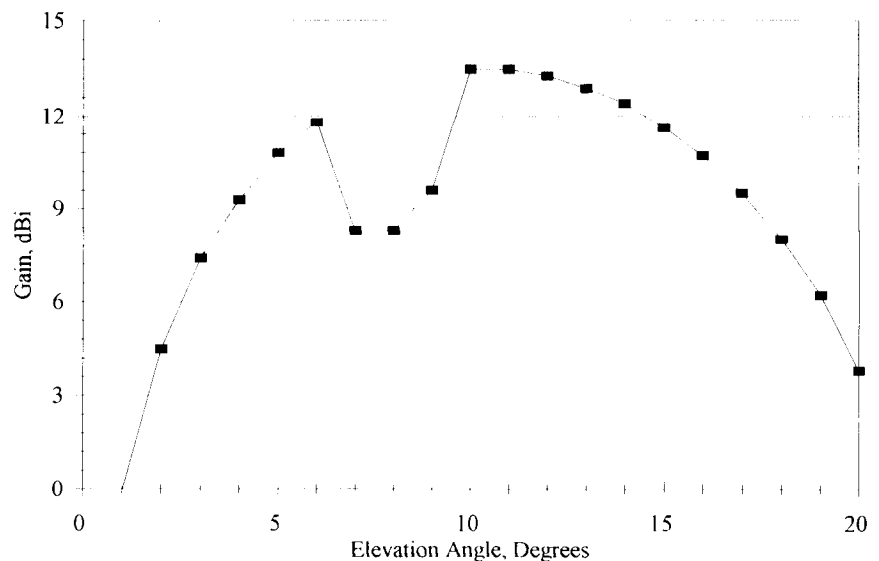


Fig 6—Elevation response for rays launched at terrain in Fig 5 from a height of 60 feet using a four-element Yagi. This was computed using a simple Geometrical Optics (GO) reflection-only analysis. Note the “hole” in the response between 6° to 10° in elevation. It is not reasonable for a 10-foot-high rock to create such a disturbance at 21 MHz!

Simulation of Reality— Some Simple Examples First

I want to admonish the reader to take care—the computer is a tool for simulation of reality, but it always has limitations built into it. A simulation of reality is exactly that, a simulation. It is only as “real” as the assumptions behind the software driving the simulation. The plain fact is that the good Lord made the world a *very* complicated place. We human beings have to make simplifying assumptions before we can even attempt to understand what we see around us.

So, please retain some degree of healthy skepticism about whatever pops out of a computer program. Use your common sense and experience to filter the results! Later on, I'll go into some detail about how the *YTAD* program does what it does, but I want to focus first on some simple results, to show that the computations do make some sense.

I will present some simulations over simple terrains. I've already described the “10-foot rock at 400 feet” situation, and showed where a simple GO reflection analysis is inadequate to the task without taking diffraction effects into account.

Now look at the simple case shown in Fig 7, where a very long, continuous downslope from the tower base is shown. Note that the scales used for the X and Y axes are different: the Y-axis changes 300 feet in height (from 800 to 1100 feet), while the X-axis goes from 0 to 3000 feet. This exaggerates the apparent steepness of the downwards slope, which is actually a rather gentle slope, at $\approx -2.86^\circ$. In other words, the terrain falls 150 feet in height over a range of 3000 feet from the base of the tower.

Fig 8 shows the computed elevation response for this terrain profile, for a four-element Yagi placed on a 60-foot tower. The response is compared to that of an identical Yagi placed 60 feet above flat ground. Compared to the “flatland” antenna, the hilltop antenna has an elevation response shifted over by almost 3° towards the lower elevation angles. In fact, this shift is directly due to the -2.86° slope of the hill. Reflections off the slope are tilted by the slope. In this situation there are no diffractions, just reflections.

Look at Fig 9, which shows another simple terrain profile; I call it a “Hill-Valley” scenario. Here, the 60-foot-high tower stands on the edge of a

gentle hill overlooking a long valley. Once again the slope of the hill is exaggerated by the different X and Y-axes. Fig 10 shows the computed elevation response at 21.2 MHz for a four-element Yagi on a 60-foot-high tower at the edge of the slope.

Once again, the pattern is overlaid with that of an identical 60-foot-high Yagi over flat ground. Compared to the flatland antenna, the hilltop antenna's response above 9° in elevation is

shifted by almost 4° towards the lower elevation angles. Again, this is due to reflections off the downward slope. From 3° to 7° , the hilltop pattern is enhanced even more compared to the flatland antenna, this time by diffraction occurring at the bottom of the hill.

YTAD creates an auxiliary output file called OUT.PRN. This shows that at 5° elevation, one diffraction and two reflection components add up

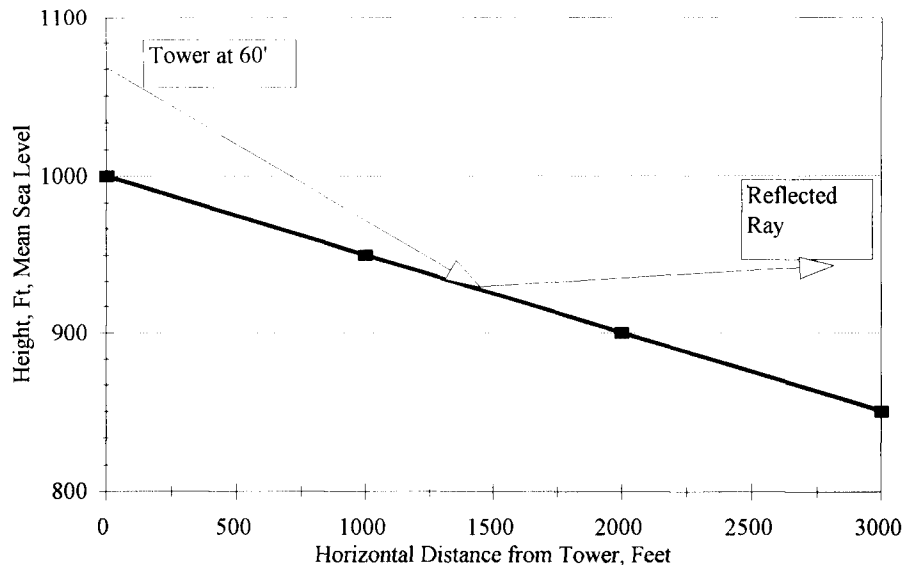


Fig 7—A long, gentle downward-sloping terrain. This terrain has no explicit diffraction points and can be analyzed using simple GO reflection techniques.

YTAD, Copyright ARRL 1995, by N6BV
HILLVALLEY.PRO ——— 60'
FLAT.PRO - - - - - 60'

Peak Gain = 16.9 dBi
21.200 MHz
21.200 MHz

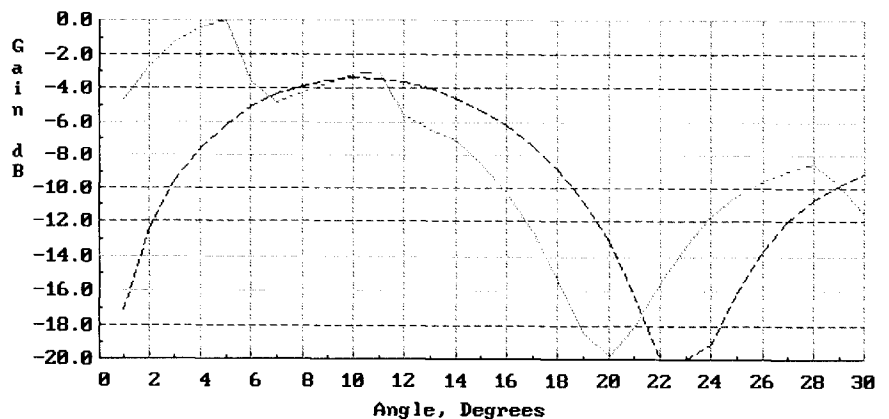


Fig 8—Elevation response for terrain shown in Fig 7, using a four-element Yagi, 60 feet high. Note that the shape of the response is essentially shifted towards the left, towards lower elevation angles, by the angle of the sloping ground. For reference, the response for an identical Yagi placed over flat ground is also shown.

vectorially to create the elevation response. Interestingly, at 4°, where the curve doesn't look particularly complicated, there are actually four components—two diffractions and two reflections—interacting with each other in the far field.

Now let's see what happens when there is a hill ahead in the direction of interest. Fig 11 depicts such a situation. Here, at a height of 400 feet above mean sea level, the land is flat in front of the tower, out to a distance 500 feet, where the hill begins. The hill then rises 100 feet over the range 500 to 1000 feet away from the tower base. After that, the terrain is a plateau, at a constant 500 feet elevation.

Fig 12 shows the computed elevation pattern for a 4-element Yagi 60-foot high on the tower, compared again with an overlay for an identical 60-foot-high antenna over flat ground. The hill blocks low-angle waves directly radiated from the antenna from 0° to 2.3°. In addition, waves that would normally be reflected from the ground, and that would normally add in phase from about 2.3° to 10°, are blocked by the hill also. Thus the signal at 8° is down almost 8 dB from the signal over flat ground, all due to the effect of the hill. Diffracted waves start kicking in once the direct wave rises enough above the horizon to illuminate the top edge of the hill. These diffracted waves tend to augment elevation angles above about 8°, which reflected waves can't reach.

Is there is any hope for someone in such a lousy QTH for DXing? Fig 13 shows the elevation response for a truly heroic solution. This involves a stack of four 4-element Yagis, mounted at 120, 90, 60 and 30 feet on the tower. Now, the total gain is just about comparable to that from a single 4-element Yagi mounted over flat ground. Where there's a will, there is a way!

At 5° elevation, four diffraction components add up (there are zero reflection components) to achieve the far-field pattern. This seems reasonable, because each of the four antennas is illuminating the diffraction point separately and we know that none of the four antennas can "see over" the hill directly to produce a reflection at a low launch angle.

You will note something new on Fig 13—another curve has appeared. The line with asterisks refers to the legend "W1-EUROP.PRN." This curve portrays the relative percentage of time during which a particular eleva-

tion angle arrives in New England from Europe. We have thus integrated on one graph the range of elevation angles necessary to communicate from New England to Europe (over the whole 11-year sunspot cycle) with the response attributed to the topography of a particular terrain.

For example, at an elevation angle of 5°, 15-meter signals arrive from

Europe about 19% of the total number of times when the band is actually open. We can look at this another way. For about two-thirds of the times when the band is open on this path, the incoming angle is between 3° to 8°. For about one-quarter of the time, signals arrive above 10°, where the four-stack is finally beginning to come into its own, sort of, anyway.

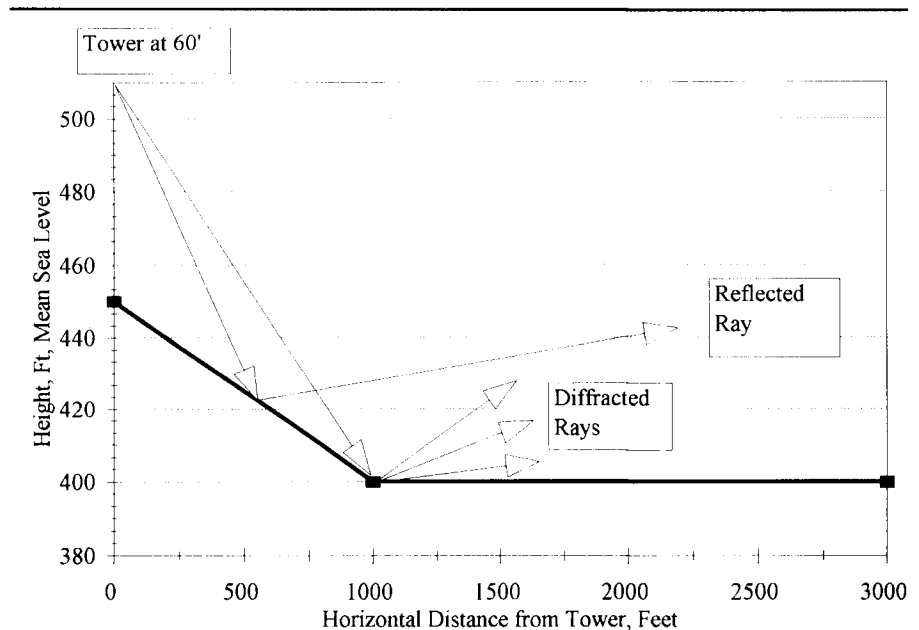


Fig 9—"Hill-valley" terrain, with reflected and diffracted rays.

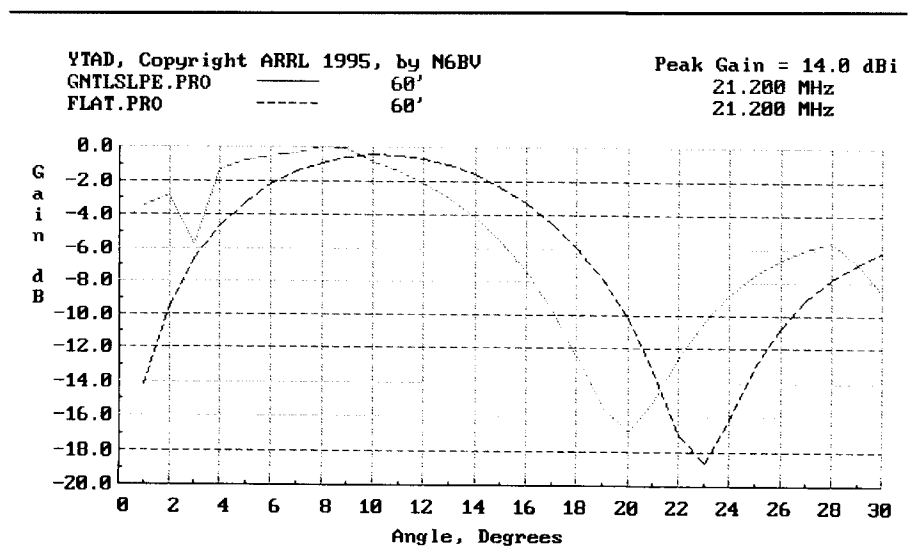


Fig 10—Elevation response computed by YTAG program for single four-element Yagi at 60 feet above "Hill-valley" terrain shown in Fig 9. Note that the slope has caused the response in general to be shifted towards lower elevation angles. At 5° elevation, the diffraction components add up to increase the gain slightly above the amount a GO-only analysis would indicate.

A More Complex Terrain

The results for simple terrains look reasonable; let's try a more complicated real-world situation. Fig 14 shows the terrain from my own QTH towards Japan. The terrain is complex, with 17 different points *YTAD* identifies as diffraction points. Fig 15 shows the *YTAD* output for three different types of antennas on 20 meters: my stack at 120 and 60 feet, the 120-foot antenna by itself, and then a 120-foot high antenna over flat ground, for reference. The elevation-angle statistics for New England to the Far East (Japan) are overlaid on the graph also, making for a very complicated looking picture—it is a *lot* easier to decipher the lines on the color CRT, by the way, than on a black-and-white printer.

Examination of the detailed data output from *YTAD* shows that at an elevation angle of 5°, the peak percentage angle (23% of the time when the band is open), there are three reflection components for the 120/60-foot stack, but there are also 25 diffraction components! There are many, many signals bouncing around off my terrain on their trip to Japan. Note that because of blockage of some parts of the terrain, the 60-foot high Yagi cannot illuminate all the diffraction points, while the higher 120-foot Yagi is able to "see" these diffraction points.

It is fascinating to reflect on the thought (sorry, I couldn't resist the pun) that received signals coming down from the ionosphere to the receiver are having encounters with my terrain, but from the opposite direction. It's not surprising, given these kinds of interactions, that transmitting and receiving might not be totally reciprocal.

I find it interesting that the 120/60-foot stack, indicated by the light solid line in Fig 15, achieves a gain of 14.7 dBi at 12° elevation, where it is about 6 dB stronger than the single 120-foot high four-element Yagi. At 11° elevation, the difference is about 13 dB in favor of the stack. At times, I have actually observed such a marked difference in performance between the stack and each antenna by itself. Such performance differences due to complex terrain may in fact partly account for why stacks often seem to be "magic" compared to single Yagis at comparable heights.

Certainly there is no way a two-beam stack can actually achieve a 13 dB difference in gain over a single

antenna due to stacking alone. Computer modeling over flat ground indicates a maximum practical gain difference on the order of 2.5 to 3 dB, depending on the spacing and interaction between individual Yagis in a stack of two.

At other times, I have seen very little difference between the stack and an individual Yagi from the stack. This occurs when the opening to Japan is occurring at a low launch angle.

When the elevation angle is 5°, for example, *YTAD* computes that the difference between the 120/60-foot stack and the single 120-foot antenna is only 2 dB. This is too small a difference to measure meaningfully, especially when the QSB varies signals by 20 dB or so during a typical QSO.

What Makes *YTAD* Tick?

Generating a Terrain Profile

It's now time for some details about

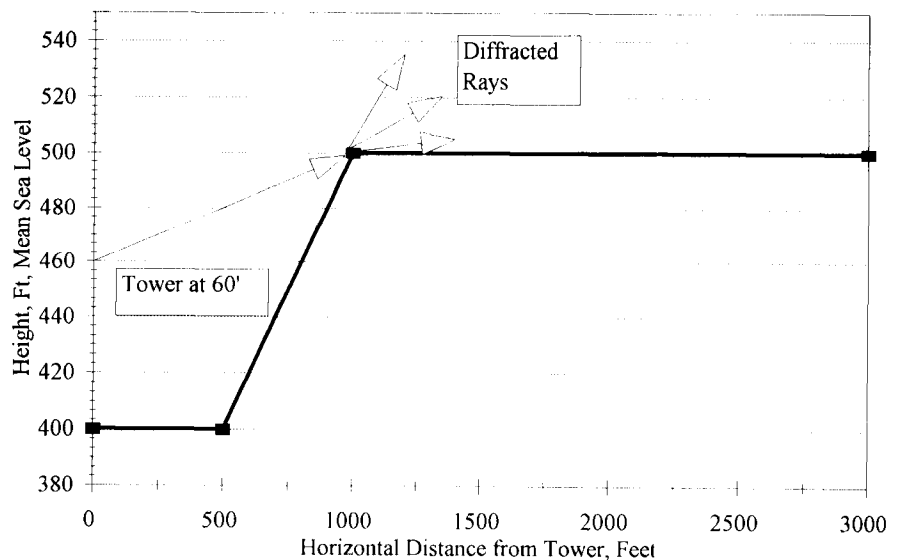


Fig 11—"Hill-ahead" terrain, shown with diffracted rays created by illumination of the edge of the plateau at the top of the hill.

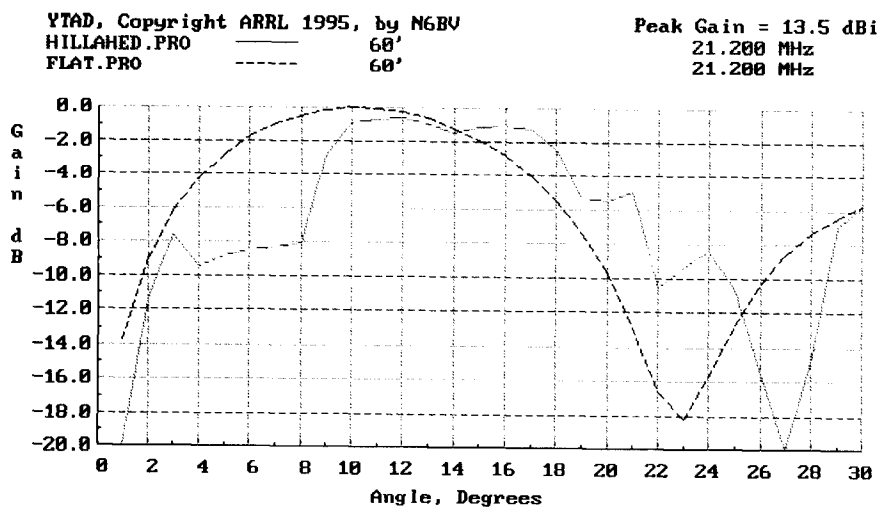


Fig 12—Elevation response computed by *YTAD* for "Hill-ahead" terrain shown in Fig 11. Now the hill blocks direct rays and also precludes possibility of any constructive reflections. Above 10°, diffraction components add up together with direct rays to create the response shown.

how *YTAD* works. As mentioned previously, the heart of the program uses two distinct algorithms to generate the far-field elevation pattern. The first is a simple reflection-only Geometric Optics (GO) algorithm. The second is the diffraction algorithm using the Uniform Theory of Diffraction (UTD). These algorithms work with a digitized representation of the terrain profile for a single azimuthal direction—for example, towards Japan or towards Europe.

The terrain file is generated manually using a topographic map and a ruler or a pair of dividers. The *YTAD.DOC* file included in *YTAD.ZIP* gives complete instructions on how to create a terrain file. The process is simple. Mark on a US Geological Survey 7.5-minute map the exact location of your tower. You will find 7.5-minute maps available from some local sources, such as large hardware stores, but the main contact point is the US Geological Survey, Denver, CO 80225 or Reston, VA 22092. Ask for the folder describing the topographic maps available for your geographic area.

Mark off a pencil line from the tower base, in the azimuthal direction of interest, perhaps 45° from New England to Europe or 335° to Japan. Then measure the distance from the tower base to each height contour crossed by the pencil line. Enter the data at each distance/height into a computer file, whose filename extension is "PRO," standing for "profile."

Fig 16 shows a portion of the USGS map for my QTH in Windham, NH, along with lines scribed in several directions towards various parts of Europe and the Far East. Note that I had to manually label the elevation heights of the contour lines in order to make sense of things. It is very easy to get confused unless you do this.

The terrain model used by *YTAD* assumes that the terrain is represented by flat "plates" connecting the elevation points in the *.PRO file with straight lines. The model is two dimensional, meaning that range and elevation are the only data for a particular azimuth. In effect, *YTAD* assumes that the width of a terrain plate is wide relative to its length. Obviously, the world is three dimensional. If your shot in a particular direction involves aiming your Yagi down a canyon with steep walls, then it's pretty likely that your actual elevation pattern will be different than what *YTAD* tells you. The signals will have to careen hori-

zontally from wall to wall, in addition to being affected by the height changes of the terrain. *YTAD* isn't designed to do canyons.

To get a true 3-D picture of the full effects of terrain, a terrain model would have to show azimuth, along with range and elevation, point-by-point for about a mile in every direction around the base of the tower. Believe me, after you go through the

pain of manually creating a profile for a single azimuth, you'll appreciate the immensity of the process if you were you try to create a full 360° 3-D profile!

Some may say that digital terrain maps are available. That is true, but let me caution you that the digitized data I have examined from several such databases is fairly crude in terms of resolution. I imagine that the data

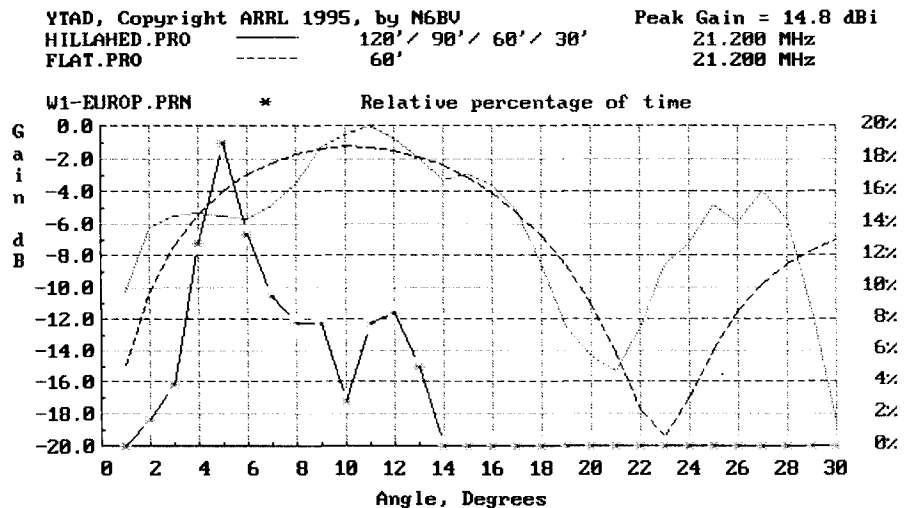


Fig 13—Elevation response of "heroic effort" to surmount the difficulties imposed by hill in Fig 11. This effort involves a stack of four 4-element Yagis in a stack starting at 120 feet and spaced at 30-foot increments on the tower. The response is roughly equivalent to a single four-element Yagi at 60 feet above flat ground, hence the characterization as being a "heroic effort."

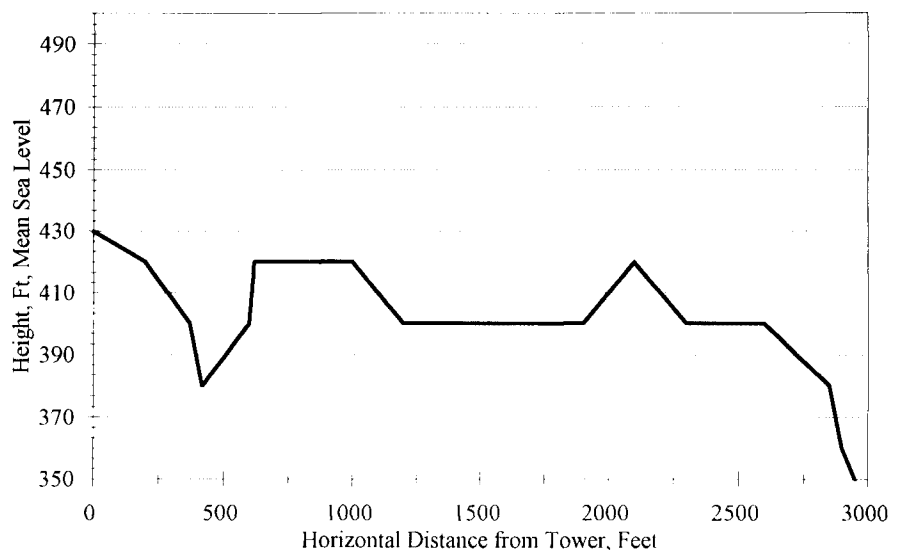


Fig 14—Terrain of N6BV in Windham, NH, towards Japan. *YTAD* identifies 17 different points where diffraction can occur.

is adequate to keep a cruise missile flying above the terrain, one of the original intents for digitized terrain data, and the data is no doubt adequate for many other nonmilitary purposes too. But I doubt that it is sufficiently detailed to be truly representative of what your antenna looks down at from the tower. Those of you with access to such digital data, try it for yourself and then compare the results with a detailed profile you generate by hand. I'd love to hear some feedback.

Algorithm for Ray-Tracing the Terrain

There are a number of mechanisms that should be taken into account as the ray travels over the terrain:

1. classical ray reflection, with Fresnel ground coefficients;
2. direct diffraction, where a diffraction point is illuminated directly by a Yagi, with no intervening terrain features blocking the direct illumination;
3. when a diffracted ray is subsequently reflected off the terrain;
4. when a reflected ray encounters a diffraction point and causes another series of diffracted rays to be generated; and
5. when a diffracted ray hits another diffraction point, generating another whole series of diffractions. This mechanism sounds a little like infinity multiplied by infinity...it is not modeled by *YTAD*.

Certain unusual, bowl-shaped terrain profiles, with sheer vertical faces, can conceivably cause signals to reflect or diffract in a backwards direction, only to be reflected back again in the forward direction by the sheer-walled terrain to the rear. *YTAD* does not accommodate these interactions, mainly because to do so would increase the computation time more than I like. As it is, terrains such as that of my own QTH into Japan take five to six seconds long to compute when I model three antennas in a stack, even on a 486DX-33 computer. This seems just barely tolerable to me as an operator.

Whenever the internal diffraction matrices in *YTAD* are filled, meaning that more than 2000 diffraction components are involved, a message will come on-screen warning that this is happening. I've only seen this message appear for exceedingly complex terrains, with stacks of three or more Yagis. If this message should appear, be wary of the computations, because some diffraction components are being ignored.

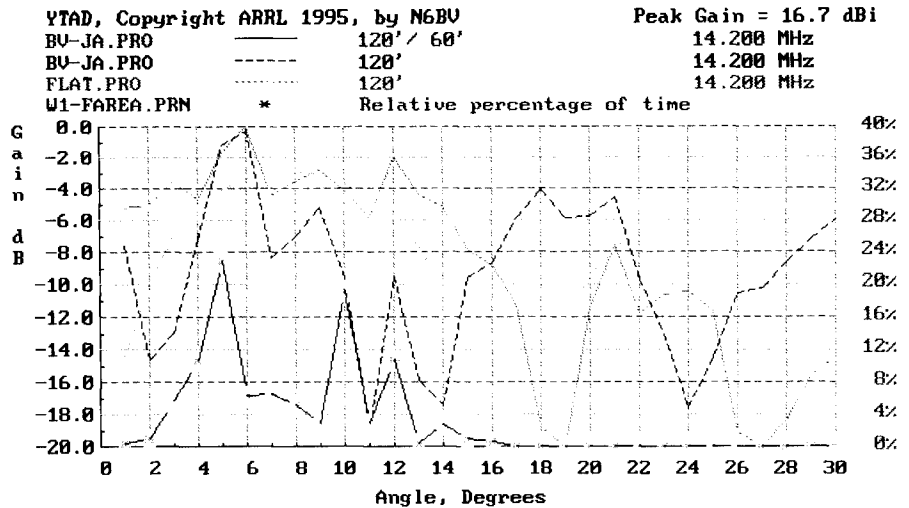


Fig 15—Elevation responses computed by *YTAD* for N6BV terrain shown in Fig 14, for a stack of two 4-element Yagis at 120 and 60 feet, together with the response for a single Yagi at 120 feet. The response due to many diffraction and reflection components is quite complicated! The response for a single four-element Yagi over flat ground is shown by the light dotted line, for reference.

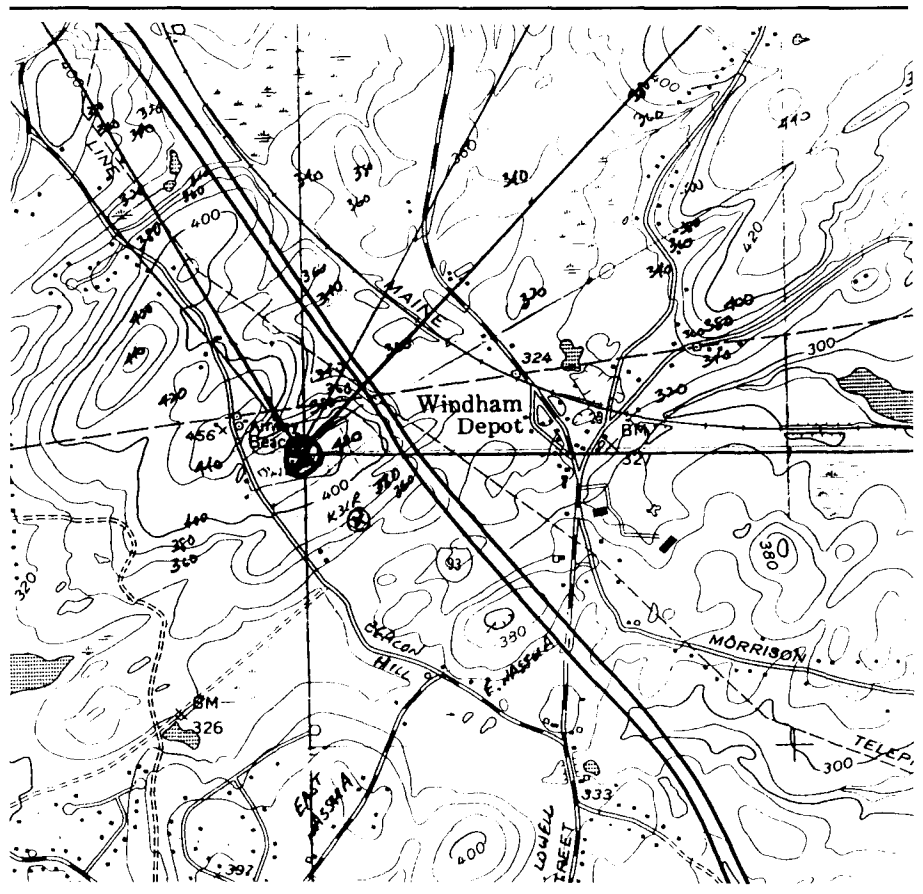


Fig 16—A portion of USGS 7.5-minute topographic map, showing N6BV QTH, together with marks in direction of Europe and Japan from tower base. Note that the elevation contours were marked by hand to help eliminate confusion. This required a magnifying glass and a steady hand!

YTAD's Internal Antenna Model

The antenna modeled inside *YTAD* assumes a simple cosine-squared response, equivalent to a four-element Yagi in free space. Why a four-element Yagi? First of all, I use TH7DX tribanders at my QTH, and they are roughly equivalent to a four-element design, with traps.

YTAD traces rays only in the forward direction from the tower along the azimuth of interest. This keeps the algorithms reasonably simple and saves computing time, while minimizing memory requirements. Since the Yagi model assumes that the antenna has a decent front-to-back ratio, I don't have to worry about signals bouncing off the terrain behind the tower, something I'd definitely have to be concerned with for a dipole, for example.

YTAD considers each Yagi in a stack as a separate point source. The simulation begins to fall apart if a traveling wave type of antenna like a rhombic is used, particularly if the terrain changes under the antenna—that is, the ground is not flat under the entire antenna. This was brought home to me when Lew Gordon, K4VX, and I tried to model his terrain ahead of, and around, his huge rhombic. For a typical Yagi, even a long-boom one, the point-source assumption is reasonable.

The internal antenna model also assumes that the Yagi is horizontally polarized. *YTAD* does not do vertically polarized antennas. I want to mention at this point that Brian Beezley, K6STI, has created a program similar to *YTAD*. He calls his program *TA*, standing for "Terrain Analysis."

Early on, I shared with him some of the Ohio University FORTRAN code for diffraction analysis, and he subsequently shared with me many valuable insights about diffraction modeling. Brian has been a good friend for years, and he's also a good friend of the League. He provided several of his programs to the League for use with antenna publications I worked on, namely *The ARRL Antenna Book* and *The ARRL Antenna Compendium, Vol 4*.

Brian's *TA* program is far more full-featured than *YTAD*, and the user-interface is decidedly more elegant than that my character-based *YTAD*. With a mouse, the *TA* user can move various parts of the terrain around to see the effects on the elevation response in the far field. *TA* also takes into account more diffraction mechanisms than

does *YTAD*, and it models vertically polarized antennas.

TA can also use the pattern output generated by K6STI's other antenna modeling programs, allowing the overall response for virtually any type of antenna to be modeled over whatever terrain the operator chooses. This means, for example, that a dipole or vertical array can be modeled over any terrain, and *TA* will compute the response both frontwards and backwards.

TA compares well with the measurements described earlier as done by Jim Breakall, WA3FET, by helicopter in Utah. Breakall's measurements were done with a 15-foot-high horizontal dipole and a vertical monopole. As I just explained, *YTAD* models neither of these antenna types particularly well, so I can't run direct comparisons between Breakall's measurements and *YTAD*. However, comparisons between *YTAD* and *TA* over the Utah terrain, when both programs used a four-element Yagi 15 feet off the ground, yielded very comparable results.

Of course, there are also a few things that *YTAD* does that *TA* doesn't yet do, including the integration of the statistical elevation-angle data from *The ARRL Antenna Book* diskette with the computed elevation response. Because I love multiple stacked Yagis, *YTAD* also models stacks of up to four identi-

cal four-element Yagis. Overall, however, since both programs have different sets of features, I think they complement each other well.

More Details About YTAD Frequency Coverage

Several people have asked me whether *YTAD* can be used on frequencies higher than the HF bands. I see no reason why it can't be used, providing that the user realizes that the graphical resolution is only a degree. The patterns above about 100 MHz would look less "grainy" if the resolution were less. But the UTD is a "high-frequency asymptotic" solution, so in theory the results get more realistic as the frequency is raised.

Keep in mind too that *YTAD* is designed to simulate launch angles for skywave propagation modes. This would include F-layer and even Sporadic E. Since by definition the launch angles include only those above the horizon, direct line-of-sight UHF modes involving negative launch angles are not considered.

Computer Hardware Required

Out of morbid curiosity, I broke out an ancient boat-anchor 4.77-MHz, 8088 computer, with an 8087 numeric coprocessor installed and 640K of RAM, and used it to run *YTAD*. A computation that my 486DX-33 completed in about 6 seconds took 3 minutes, 59

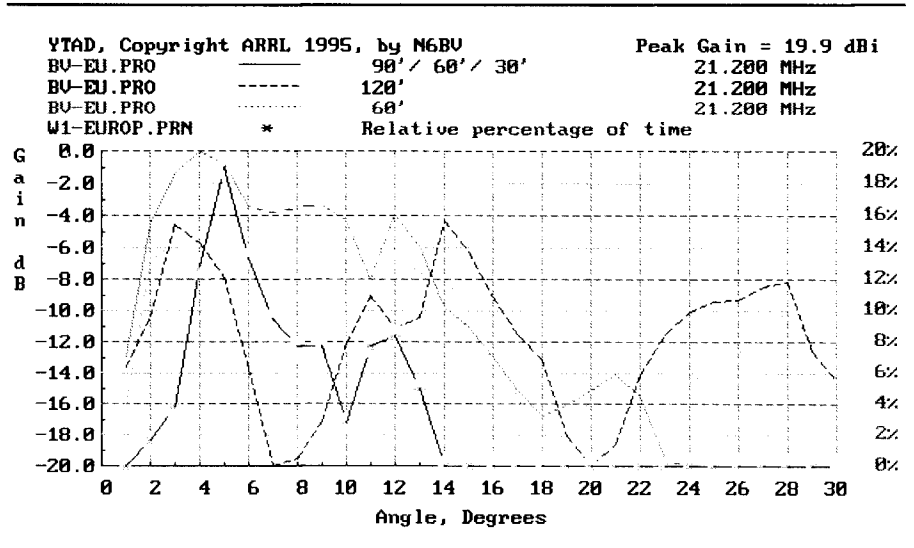


Fig 17—Computed elevation responses for N6BV terrain towards Europe, for three antennas: a stack at 120/60 feet, a single antenna at 120 feet, and a single antenna at 60 feet. From monitoring BBC at 21470 kHz and switching rapidly between the various antennas, I determined that predominant angle of elevation in June 1995 was about 2° to 3°.

seconds to do. The graph also wouldn't show on-screen properly, because *YTAD* will only display graphics on an EGA or a VGA display adapter.

Then I got a little more frisky, and I disabled the 8087 coprocessor. I got a good snore out of that exercise, because after an hour and 40 minutes it finally finished. There's a moral to this story. If you want to use software like *YTAD*, which crunches a whole lot of numbers, use a fast machine and use one with a numeric coprocessor. Otherwise, you'll get old before your time, as you wait impatiently for something to happen!

Where Can You Get *YTAD*, and What Do I Want in Return?

YTAD is an experimental work-in-progress. As such there is presently no charge for *YTAD*. The program is available as *YTAD.ZIP* on the ARRL Hiram BBS at 203-594-0306. The zipped file contains the *YTAD.EXE* program, plus the *YTAD.DOC* documentation file and a number of sample terrain profiles.

If you are on Internet, you can get *YTAD.ZIP* by anonymous FTP from ftp.cs.buffalo.edu in the /pub/ham-radio/qex directory. If the last bit of Internet alphabet soup didn't make any sense to you, you can also send me a formatted IBM 3.5-inch floppy disk with a stamped return-mailer envelope and I'll mail back your disk to you with *YTAD.ZIP* on it.

What I'd like in return is validation data for the results computed by *YTAD* for your QTH. I don't expect you to hire a helicopter and a team of dedicated scientists to generate validation data, but for those of you with access to stacked antennas, the methodology shown in Fig 15 may be useful. On a well-calibrated receiver S-meter, the difference in response for the Yagis at various heights may be used to judge whether the *YTAD* simulation is reasonable or not, especially when coupled with the statistical range of elevation angles that can be expected

for a particular path. You will have to switch between various antennas quickly, trying to minimize the effects of QSB.

I use the broadcast stations just above the 15-meter band as beacons for making just such tests. I do have to be careful to recognize where the transmitting station is actually located. For example, the BBC very often transmits from Ascension Island rather than from London. It is very helpful to have a list of times/frequencies/transmitting locations for the SWLing you do in your validation quest.

For example, this morning as I sit writing this article, I am monitoring BBC from Cyprus on 21470 kHz. My stack of three TH7DX tribanders at 90/60/30 feet is just about equal to the single 4-element 714X-3 tribander at 120 feet; the 120-foot antenna is just slightly stronger than the single 60-foot TH7DX. See Fig 17 for a screen print of what *YTAD* computes for these combinations. The most likely elevation angle reflecting these signal levels falls between 2° to 3° even though the likelihood for this is only about 6%. I ran a computation using *CAPMAN*¹² for SSN = 10 in the month of June and this confirmed that the elevation angle would indeed be very low, in the region of 2°.

A Final Note

One last word: How would I estimate the "accuracy" of *YTAD* computations? Frankly, I would not be willing to bet money that the accuracy is better than ±3 dB. Of course, I actually believe the program is more accurate than ±3 dB, based as it is on solid theoretical grounds—it's just that I wouldn't bet a lot of money on it!

It is difficult to validate *YTAD* computations on a truly scientific basis, other than the aforementioned technique requiring a helicopter equipped with lots of test gear. I would definitely recommend however that the reader *not be obsessive*, trying to fiddle with

the heights of your antennas in tiny increments hoping to gain tiny advantages at certain angles! I trust you have better things to do with your life, like talk with your families or work DX or contests.

I hope that *YTAD* and programs like it will prove useful to the amateur fraternity, helping us choose not only our QTHs, but also our antenna configurations on a more scientific basis.

Notes

- ¹Burke, G. J. & Poggio, A. J., "NEC2, Numerical Electromagnetics Code—Method of Moments," NOSC Technical Document 116, 1981. Distributed by NTIS, Springfield, VA 22161.
- ²Logan, J. C., Rockway, J. W., "The New MININEC (Version 3): A Mini-Numerical Electromagnetic Code," Tech Doc 938, Naval Ocean Systems Center, San Diego, 1986.
- ³*NEC/Wires*, by Brian Beezley, K6STI, 3532 Linda Vista Dr, San Marcos, CA 92069.
- ⁴*EZNEC*, by Roy Lewallen, W7EL, PO Box 6658, Beaverton, OR 97007.
- ⁵*YO* by Brian Beezley, K6STI, 3532 Linda Vista Dr, San Marcos, CA 92069.
- ⁶*YagiMax*, by Lew Gordon, K4VX, PO Box 105, Hannibal, MO 63401.
- ⁷Michaels, Charles J., W7XC, "Horizontal Antennas and the Compound Reflection Coefficient," *The ARRL Antenna Compendium, Volume 3* (Newington: ARRL, 1990), pp 175-184.
- ⁸Breakall, J. K., Young, J. S., Hagn, G. H., Adler, R. W., Faust, D. L., and Wernerm D. H., "The Modeling and Measurement of HF Antenna Skywave Radiation Patterns in Irregular Terrain," *IEEE Transactions on Antennas and Propagation*, Vol 42, No. 7, July 1994.
- ⁹McNamara, D. A., Pistorius, C. W. I., Malherbe, J. A. G., *Introduction to the Uniform Geometrical Theory of Diffraction* (Boston: Artech House, 1994).
- ¹⁰Keller, J. B., "Geometrical Theory of Diffraction," *Journal Opt. Soc. Amer.*, Vol. 52, 1962, pp 116-130.
- ¹¹Kouyoumjian, R. G. and Pathak, P. H., "A Uniform Geometrical Theory of Diffraction for an Edge in a Perfectly Conducting Surface," *Proc. IEEE*, Nov 1974, pp 1448-1461.
- ¹²*CAPMAN*, available from LUCAS Radio/Kangaroo Tabor Software, 2900 Valmont Rd, Suite H, Boulder, CO 80301, tel 303-494-4647. □

Spectral Measurements the Hard Way

*When the easy way — a spectrum analyzer —
isn't available, the hard way is the easy way!*

By John C. Reed, W6IOJ

The rapid growth of activity in the VHF/UHF spectrum has emphasized the need for spectral purity of transmitters and receivers. The experimenter, who often uses junk box parts and innovative designs, is particularly vulnerable to making equipment with unpredictable spectral performance. One problem is that spurious signal-performance measurements are difficult to make without the use of a spectrum analyzer, an expensive instrument that is often unavailable to the experimenter.

This article describes a direct-conversion receiver configured to perform as a spectrum analyzer. Although the method has limitations, the performance data shows that it provides reasonable spurious response data up to -80 dB in the 3.5-MHz to 1.3-GHz frequency range. The relatively simple circuitry is mounted on two circuit boards contained in a 3×5¹/₄×5⁷/₈-inch metal cabinet. The system requires the use of outboard plug-in attenuators and a local oscillator.

General Description

Referring to the block diagram, Fig 1, the signal to be

measured is applied to one input of a product detector and a local oscillator source to the second input. A 25-kHz detector reference-level output is established by applying a local oscillator (LO) source at a frequency 25 kHz different from that of the input signal. This is amplified in the preamplifier and postamplifier to a convenient level for processing.

A 25-kHz filter follows. Its output is peak-detected and the level is monitored by a meter calibrated in 3-dB steps, with full scale representing a 0-dB reference.

An audio monitor capability is provided with an additional detector together with a 25-kHz beat-frequency oscillator (BFO) for conveniently detecting spurious responses. It is particularly useful when searching for low-level signals.

An optional filter output has been included for external oscilloscope monitoring. A measurement is made by increasing the postamplifier gain with the panel rotary selector switch and tuning the LO frequency to a frequency having a spurious response. It should be noted that the LO level can vary between 5 mW and 100 mW without affecting the reference calibration. That is, different LOs can be plugged in while maintaining the same calibration.

Once peaked to the spurious response, the gain is reduced by the calibrated panel rotary switch to make the meter

770 La Buena Tierra
Santa Barbara, CA 93111-1705
email: reedioj@aol.com

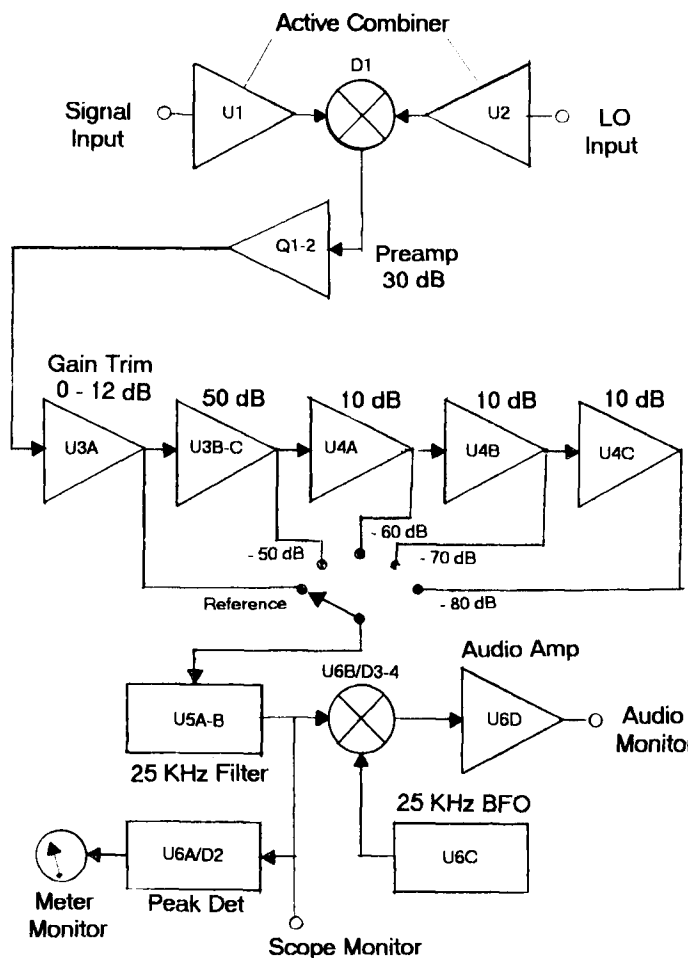


Fig 1—Block diagram of the analyzer.

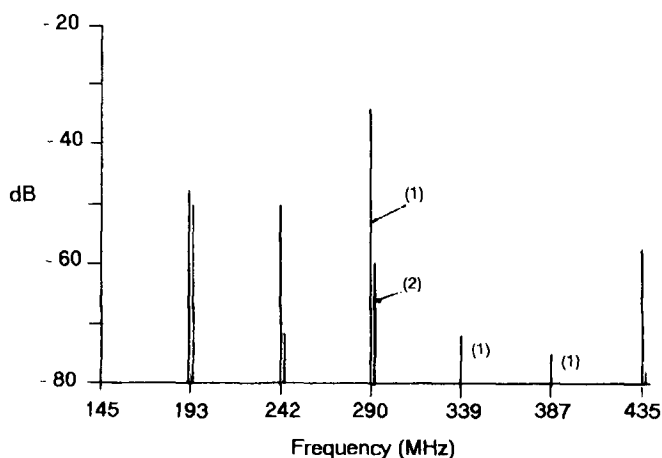


Fig 3—Measured response of a 145-MHz source. (1) Multistage VXO, 16/48/145 MHz. (2) Additional single-section low-pass filter; the response is less than -80 dB at 339 and 387 MHz.

output full scale or less. A combination of the switch position and meter reading indicates the spurious response level. If the spurious response is stronger than -50 dB (the limit of the calibrated rotary switch), an additional attenuator in the input scales the results accordingly. As an example, adding a 20-dB attenuator will make the selector rotary switch calibration 30 to 60 dB. Examples of the operating results are shown in Fig 2 (3.5 MHz), Fig 3 (145 MHz) and Fig 4 (435 MHz).

Design Considerations

The input signals are first processed through monolithic amplifiers that isolate the inputs by 35 dB. The isolation prevents interaction that could result in frequency pulling

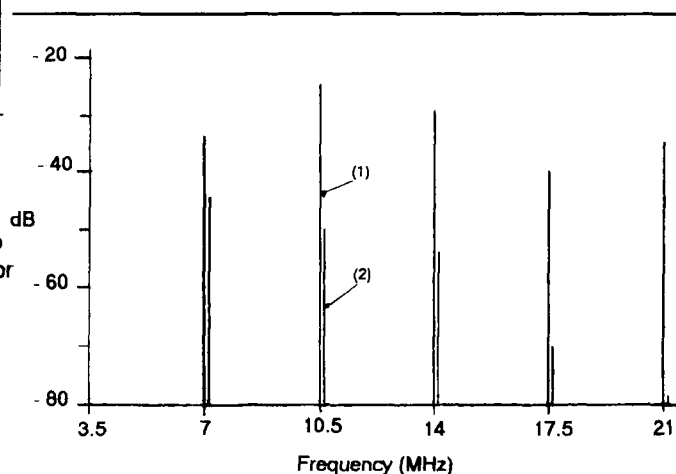


Fig 2—Measured response of a 3.5-MHz source. (1) An FET Colpitts oscillator. (2) A single-section low-pass filter added to (1).

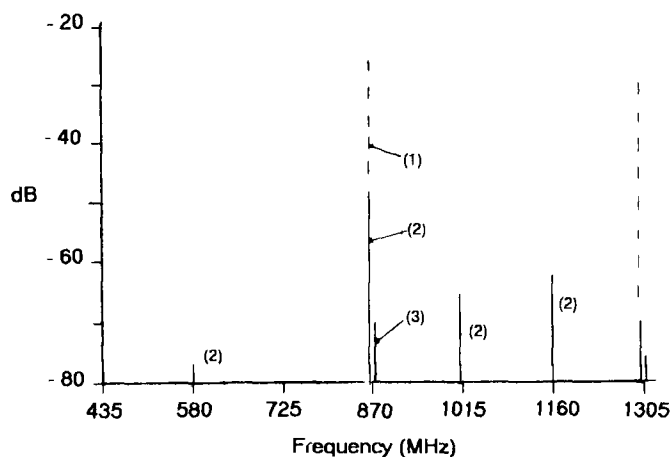


Fig 4—Measured response of a 435-MHz source. (1) Single transistor VFO. (2) Multistage source, 16/48/435 MHz. (3) Three-section 435-MHz strip-line filter added to (2); the response is less than -80 dB at 580, 1015 and 1160 MHz.

and spurious modulation products. The Mini-Circuits MAR-4 monolithic amplifier was chosen for this application, primarily because of its flat frequency response. It has a nominal gain of 8 dB with a variation of less than 0.25 dB up to 1 GHz and 1 dB up to 2 GHz. It also has a relatively high output capability, blocking at about 40 mW.

A common measurement error is caused by competitive modulation products developed from nonlinearity in the system. A conventional way of testing for this problem is to insert a 6-dB input attenuator. Analyzer nonlinearity is evident if the spurious response reading decreases by more than 6 dB. Multiorder modulation products are involved that can produce a dramatic change in the response relative to a small change in the input. As an example, lowering the input by 6 dB can make a difference between a measurement having a major error and one that is acceptable.

The maximum input signal while retaining the necessary linearity is -18 dBm ($14 \mu\text{W}$). It results in a processed output of 4-V peak-to-peak for the 0-dB reference. A -98 -dBm input signal produces the same output after adding an additional 80 dB of postamplifier gain. Under these maximum gain conditions, the S/N is about 8/1, making a -116 -dBm noise level. This results in a 20-dB system noise figure when comparing it to a 6-kHz thermal noise of -136 dBm. The NF value mainly results from combined performance of the MAR-4 amplifier, the detector assembly resistive network, the Philips ECG 584 K-Band Barrier Diode and the 3-dB penalty due to the direct conversion plus and minus outputs.

The input is adjusted close to the -18 -dBm level using a combination of 6, 10 and 20-dB plug-in attenuators. It is then trimmed to the final reference level by adjusting the panel U 3A gain control. Compensating for a weaker signal level as compared to the -18 -dBm level will increase the noise level.

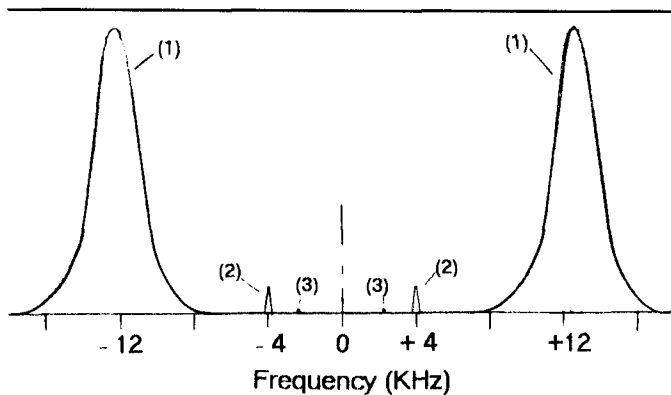


Fig 5—Output response of the 25-kHz filter. The signal frequency is $145 \text{ MHz} \pm 18 \text{ kHz}$ and the LO frequency is 290 MHz. (1) The second harmonic primary output. (2) A detector intermodulation output resulting from the 145-MHz fourth harmonic plus the LO second harmonic output. It is at a level of about -20 dB as compared to (1). (3) A detector intermodulation output resulting from the 145-MHz sixth harmonic plus the LO third harmonic output. Its level is much weaker than -80 dB and barely discernible in the audio monitor.

An important reason for processing the data through a 25-kHz filter is to minimize detector $1/f$ noise. This noise reduction, plus the improvement realized through narrowing the bandwidth from 50 to 6 kHz, decreases the noise approximately 15 dB. The effect of the 25-kHz filter is similar to that of a conventional intermediate amplifier method producing plus and minus outputs, in this case outputs that are 50 kHz apart.

However, this source difference frequency will be less when detecting a higher-order spurious response. As an example, second harmonic outputs will be 25 kHz apart. Also, detector-generated intermodulation spurious responses will appear between the two primary signals at a much lower level, -20 dB or less. The frequency of these responses will define the harmonic order causing the response. Fig 5 illustrates these conditions when specifically related to that of a second harmonic.

Hardware Notes

The detector/preamplifier circuit assembly is shown in Fig 6 and the related layout in Fig 7. With some sacrifice in performance above 500 MHz, the chip capacitors C1-6 can be replaced with parallel 470-pF disc ceramic capacitors. Reactance of RFC-1 to frequencies within the operating range will likely introduce unwanted modulation products. The molded-type ferrite choke avoids this problem. The one used in my assembly has a dc resistance of about 10Ω . The windings of T1 are operated in parallel to reduce dc resistance to about 30Ω ; substantial dc resistance in this circuit decreases the detector linear operating range. U1 and U2 each require 45 mA and the preamplifier 5 mA at 10 V.

The remaining circuitry shown in Figs 8 and 9 is mounted on a $4\frac{1}{4}$ -inch square perfbord. The following conditions are necessary to avoid feedback: a microphone-type shielded cable connects the preamplifier located on the

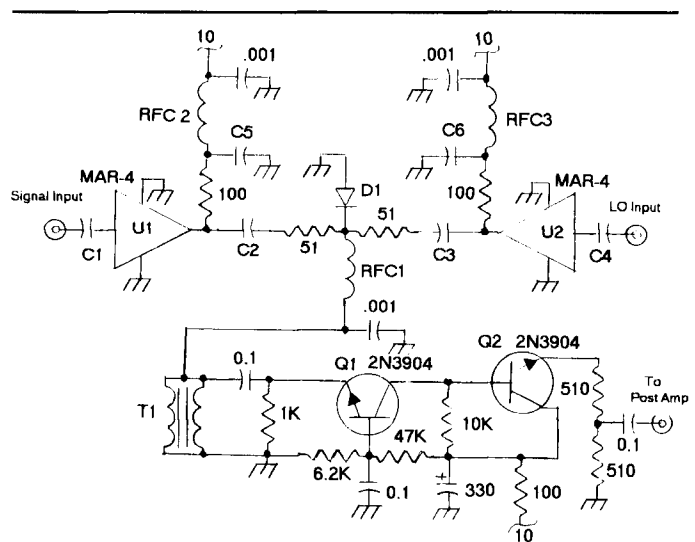


Fig 6—Schematic of the product detector/preamplifier assembly. C1-6 are 0.001 chip capacitors. U1-2 are Mini-Circuits MAR-4 monolithic amplifiers. D1 is a Philips ECG 584 Schottky barrier diode. T1 is a Radio Shack isolation transformer, RS 273-1374. RFC 1-3 are 1-mH molded chokes about $\frac{1}{16} \times \frac{3}{8}$ inches.

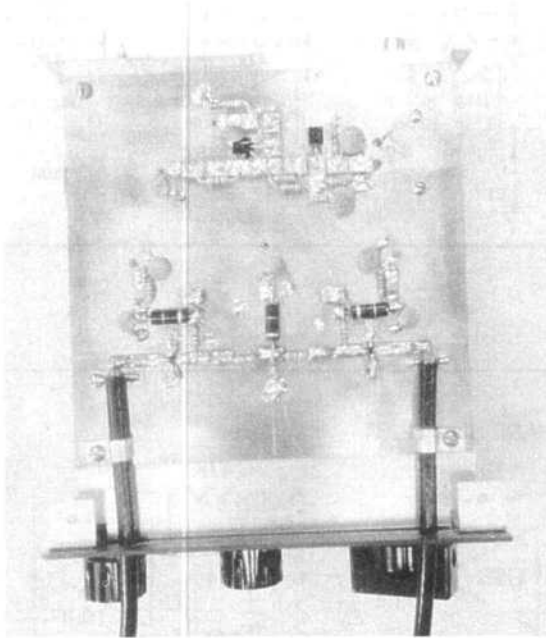
RF board to the post amplifier on the perf board. U3-4 are arranged to make minimum connecting lead lengths to the panel selector switch. Care has been taken to isolate the postamplifier as much as possible from the remaining circuitry. The complete assembly requires 125 mA at 12 to 20 V.

The plug-in attenuators are pi-network assemblies using 5% 1/4-W resistors, using the values indicated in *The ARRL Handbook*. Six-inch RG58 cables are soldered to a 1 1/2-inch square PCB such that the resistors are directly connected with minimum lead lengths. Sharply bending the

connecting lead upward allows interconnections of about 1/16 inch. The assembly is covered with a simple aluminum U-shield. The cables are terminated with twist-on BNC connectors.

Operation

The wideband detector assembly becomes inoperative in



Detector/preamp circuit board

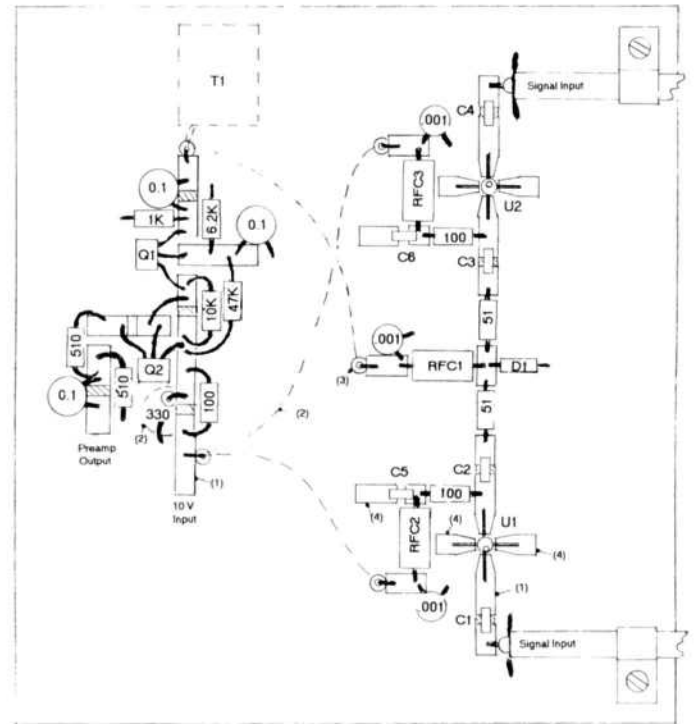
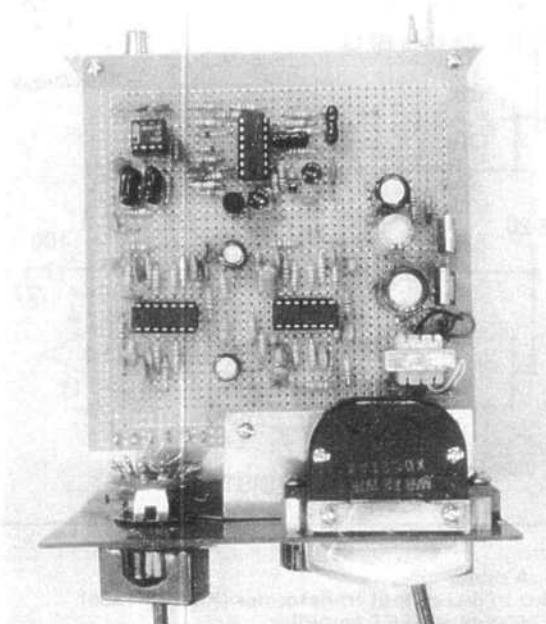
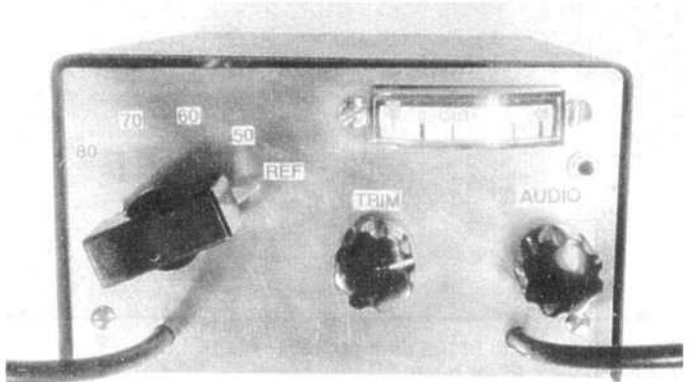


Fig 7—Layout of the product detector/preamplifier circuit board. The base PC board is 1 1/4 x 4 1/4 x 1/16-inch with foil on both sides. (1) Glue-down 1/8-inch wide PCB strips. Cross-hatch marks indicate areas where the foil has been removed. Strips are glued down with a clear cement. (2) Dotted lines indicate parts mounted on the reverse side. (3) Surface of the small wire feedthrough holes are reamed out slightly to avoid possible contact between the wire and foil. (4) Grounding pads made from 0.030-inch brass. These are soldered to the base PCB.



Post amp/processor circuit board



Complete system

a strong stray radiation environment. My experience has been that acceptable performance is limited to input sources having an output of less than one watt. An RF shielded box having a capability similar to that of an RF shielded room can be a solution. The box must include the LO and the low-level attenuators.

A second limitation is difficulty in tuning the LO. In most of my testing I used single-transistor oscillators (described in June 1994 *QEX*). The self-excited oscillators need at least a half-hour warm up simply to keep the drift to within 1 kHz during a single measurement period. Also, the screw-driver frequency adjustment method does not come close to providing adequate resolution. The measurements were managed by using the audio monitor while tuning, listening for a "twerp" from the spurious response. Once close to the desired frequency, I fine tuned the source for zero-beat.

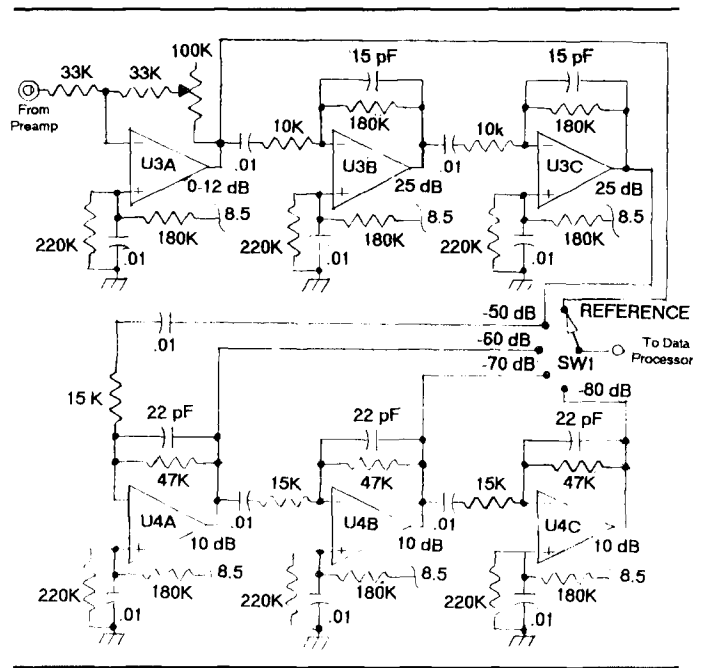


Fig 8—Schematic of the post amplifier. →
U3-4, TL084C quad JFET amplifier.
SW1, rotary switch (Radio Shack 275-1380).

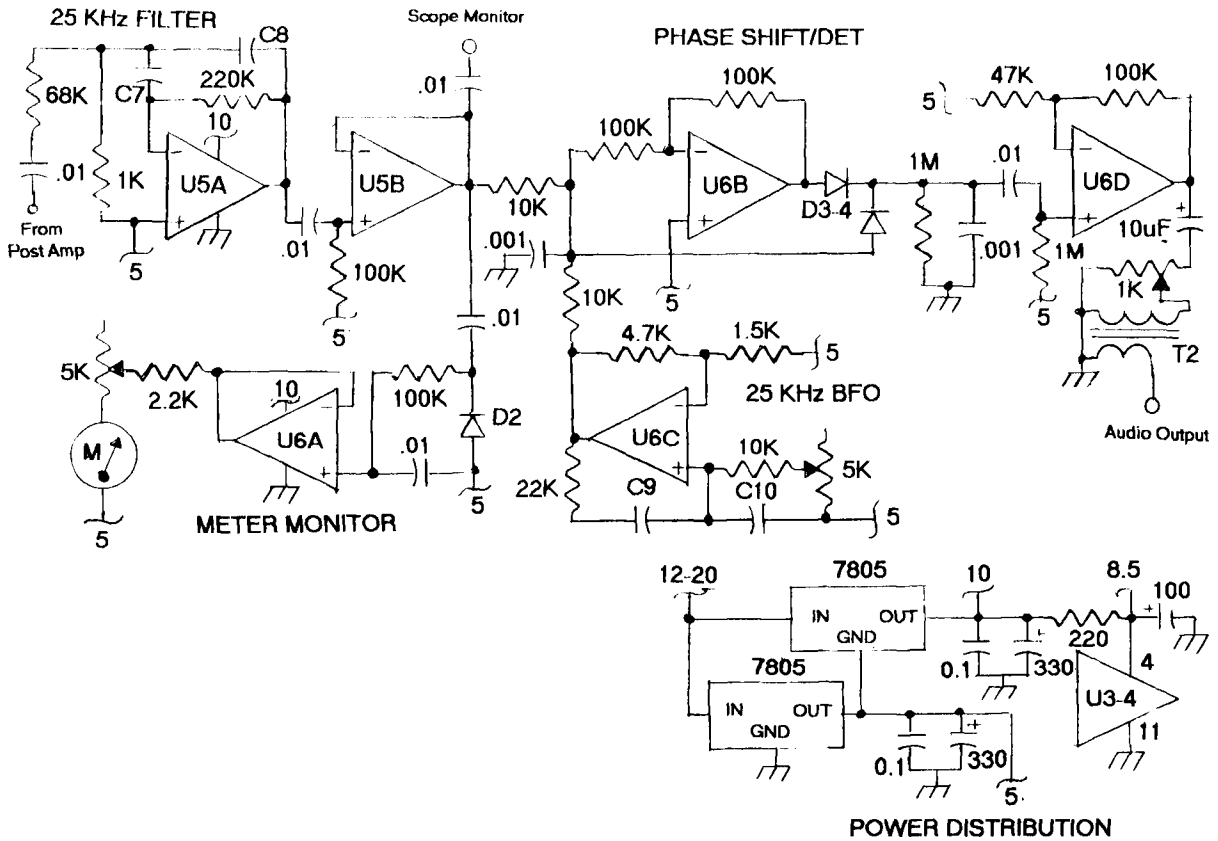


Fig 9—Schematic of the data processor.
C7-8—510-pF silver mica
C9-10—330-pF silver mica
D2—1N34A germanium diode
D3-4—1N914/1448 switching diode

M—50- μ A meter
T2—1-k Ω to 8- Ω output transformer (RS-273-1380)
U5—LF353N dual JFET amplifier
U6—TL084C quad JFET amplifier.

A Termination Insensitive Amplifier

A crystal filter input loads an amplifier with a complex impedance-versus-frequency function. This amplifier handles it.

By Jacob Makhinson, N6NWP

One of the commonly used building blocks in high-performance receivers for HF/MF reception is the post-mixer amplifier. In a traditional single-conversion receiver, the post-mixer amplifier is inserted between the mixer and the crystal filter for the purpose of improving the noise figure. The design criteria for the amplifier are very stringent:

1) the input intercept point should exceed the output intercept point of the mixer preceding the amplifier,

2) the input 1-dB compression point should exceed the output 1-dB compression point of the mixer,

3) the performance of the amplifier should not be degraded by the input impedance of the crystal filter, and

4) the input section of the amplifier

should ideally present a broadband (50 Ω) resistive termination to the mixer stage.

It is relatively easy to satisfy the first two requirements by employing a balanced version of the "lossless feedback" amplifier and providing adequate collector current.¹ It is much more difficult to satisfy the two remaining requirements, and it is the purpose of this article to show you a way to accomplish the two remaining design goals.

Recent experiments with home-built crystal ladder filters driven by a balanced lossless feedback amplifier (BLFA) revealed a serious shortcoming of this feedback implementation.^{2,3} While allowing the realization of a very low noise figure and very high intercept points, the BLFA suffers from a very high reverse feedback

inherent to its architecture. Therefore, all violent impedance variations at the input of the crystal filter, within and adjacent to its passband, are reflected back through the amplifier to the IF port of the mixer. Resistive pads at the output of the post-mixer amplifier help to "smooth down" the impedance variations, but not much. Diplexer circuits commonly used between the mixer and the post-mixer amplifier are of no use since they are low-Q circuits.

Unfortunately, most types of mixers suffer most from reactive terminations at the IF port, and the deterioration of the IM performance can be significant. Naturally a question arises: Is there a way to design an amplifier with a broadband resistive input impedance not sensitive to any variations in impedance imposed by the crystal filter on the amplifier's output?

Dr. Ulrich Rohde presented a method to solve this problem.⁴ The first section of his two-stage amplifier is a lossless feedback amplifier, and the second section is a low-impedance common-base amplifier, which accounts for the input-port immunity to impedance variations at the load terminals. The input of this amplifier is kept from being overdriven by an electronically controlled front-end attenuator. Therefore, the amplifier's IMD and the 1-dB compression point design criteria do not have to be very stringent. This architectural approach is undoubtedly quite viable in a high-performance HF/MF receiver and is bound to grow in popularity among serious-minded experimenters.

The remainder of this article describes an alternative solution. It builds upon Dr. Rohde's idea and is a fixed-gain stage strong enough to avoid being overloaded without the need to employ front-end attenuation.

Design Criteria

Measurements performed on home-built, high-performance crystal ladder filters suggest that the crystal filter may be the limiting factor in determining the IMD performance of the front end in a traditional single-conversion receiver.^{2,5} The third-order intercept

point at the input of the crystal filter can reach +46 to +47 dBm (when driven with a strong BLFA). Therefore the amplifier requires a third-order output intercept point ($IP_{3,out}$) around +50 dBm in order not to degrade the overall IMD of the front end. If the gain is set to 10 dB, the amplifier's resulting third-order input intercept point ($IP_{3,in}$) of +40 dBm is sufficient not to degrade the $IP_{3,out}$ of a commutation type mixer (+35 to +38 dBm) described in Note 3.

The 1-dB desensitization and compression points should be better than +15 dBm in order not to degrade the performance of the mixer.

If the front end is using a preamplifier, the noise figure of the post-mixer amplifier should be lower than 4 dB in order to avoid degradation of the system noise figure.

Input impedance should be 50 Ω , resistive, over a wide frequency range regardless of the nature of the output termination.

Output impedance should be adjustable from 50 Ω to 500 Ω to accommodate a wide range of crystal filters.

Circuit Description

The termination insensitive amplifier (TIA) consists of two stages (see Fig 1). The first stage is a BLFA block

similar to the one used in Note 3. It offers remarkable IMD performance (with a resistive load) considering its moderate collector current of 30 mA per transistor. At the suggestion of Colin Horrabin, G3SBI, the MRF586 transistors were replaced with MRF581. They have a lower noise figure, are less expensive and their symmetrical package with two emitter leads allows greater flexibility during construction. No dc bias adjustment is required in either stage since the IMD performance proved to be a very weak function of collector current.

Transmission-line transformer T1 acts as a balun and applies the input signal differentially to both halves of the amplifier. C1 and R1 form a frequency compensation network that ensures a flat frequency response between 2 MHz and 100 MHz. Transformers T2 and T3 set the gain of the first stage equal to 9.5 dB. R4 and R5 serve as a resistive load and have been adjusted to establish a 50- Ω impedance at the input of the amplifier. R4 and R5 are major contributors to the noise figure of the TIA, but this is the price of the termination-insensitive performance.

Transformer T4 couples the signal differentially to the second stage; it cancels out residual imbalance

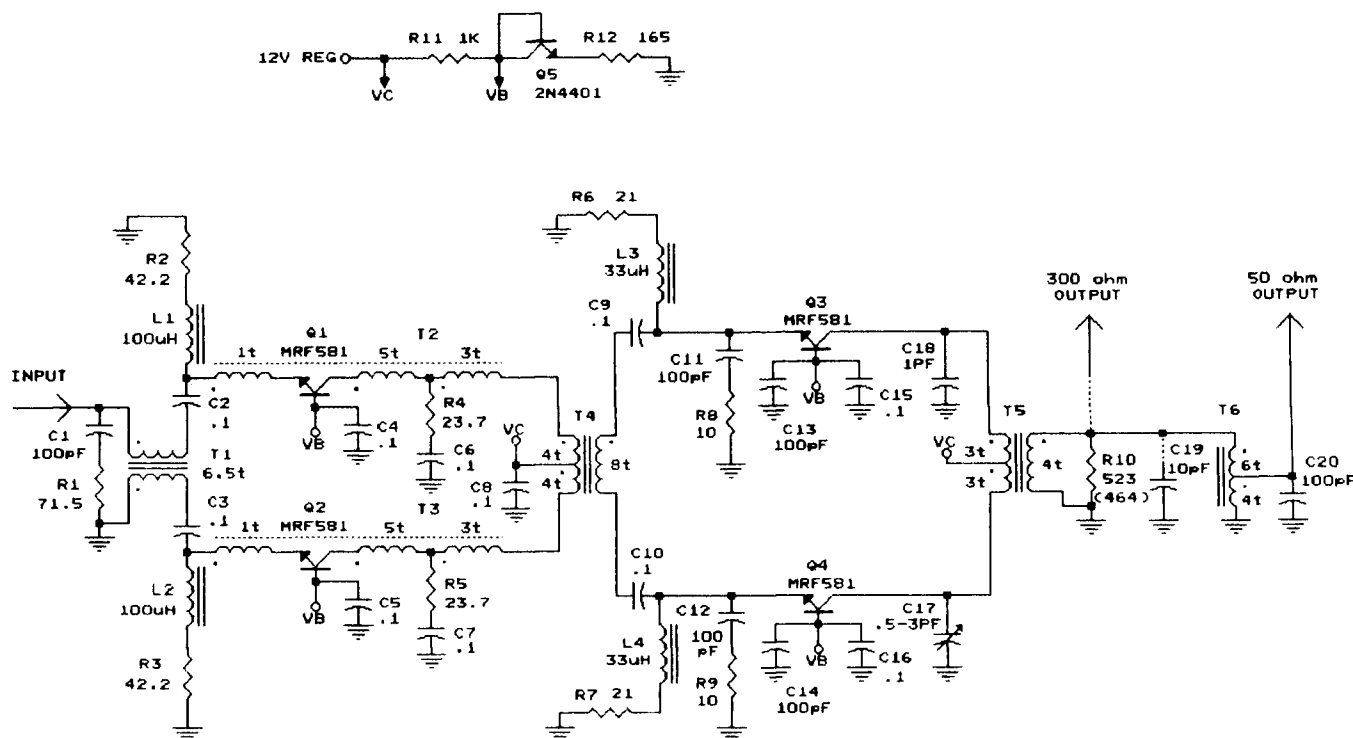


Fig 1—Schematic diagram of the TIA.

present at the output of the first stage.

The collector current of each second stage transistor is set to 50 mA to satisfy the 1-dB compression and desensitization requirements. RC networks R8-C11 and R9-C12 help to ensure stability of the stage. A pair of capacitors at the base provides a low-impedance path to ground over a wide frequency range.

The turns ratio of transformer T5 is chosen to set the overall gain to 9.5 dB (including the transformer core losses).

Capacitors C17 and C18 are included to fully realize the benefits of the balanced arrangement. Trimmer capacitor C17 cancels out any capacitive imbalance due to stray capacitances and component variations. When properly adjusted for a minimum level of the IMD products, the IP_{3out} may exceed +50 dBm.

The output signal is available at two nodes. A 50-Ω output impedance is provided at the tap of transformer T6. A higher output impedance for a direct interface with a crystal filter is available at the secondary winding of transformer T5. Transformer T5 and resistor R10 set the value of the output impedance. (The turns ratio of T5 also determines the overall gain.) The values shown in Fig 1 set the output impedance equal to 300 Ω at the secondary of T5. Component modifications required to set the output impedance to values between 100 Ω and 800 Ω are summarized in Table 1. Transformer T6 has to be disconnected or removed should the output signal be taken from transformer T5.

With the values shown, the secondary winding of T5 self-resonates at 12 MHz. Setting C19 equal to 10 pF broadly resonates the output around 8 to 9 MHz and makes the output impedance almost purely resistive.

I recommend use of the 50-Ω output during alignment and measurements since most RF measurement equipment has 50-Ω inputs. It can also be useful if 50-Ω attenuating pads are used between the TIA and the crystal filter. In this case, capacitor C19 is omitted and the value of resistor R10 is raised from 464 Ω to 523 Ω. Capacitor C20 broadly resonates T6 and makes the 50-Ω output almost purely resistive at around 8 to 9 MHz.

Network R11-Q5-R12 generates the dc bias voltage (V_B) for the transistors. Transistor Q5 provides temperature compensation for the bias voltage and is thermally coupled to the case of Q1.

A well-regulated and filtered +12-V source is required to power the amplifier. The TIA draws 160 mA from the power supply.

Construction

A two-layer PCB has been designed

to facilitate construction and to ensure performance repeatability. The components are mounted on the ground-plane side of the PCB.

It is important to remember during the construction phase that the TIA employs transistors with an f_t of

Table 1—Output impedance modification data.

Desired output impedance (ohm)	R10 for Hi-Z output (ohm)	R10 for 50 ohm output (ohm)	T5 primary (turns)	T5 secondary (turns)	T6 top (turns)	T6 bottom (turns)
100	158	162	4 + 4	3	2	5
200	348	357	4 + 4	4	4	4
300	464	523	3 + 3	4	6	4
400	634	665	4 + 4	6	9	5
500	806	931	3 + 3	5	11	5
600	976	1150	5 + 5	9	10	4
700	1100	1270	3 + 3	6	11	4
800	1370	1650	3 + 3	6	12	4

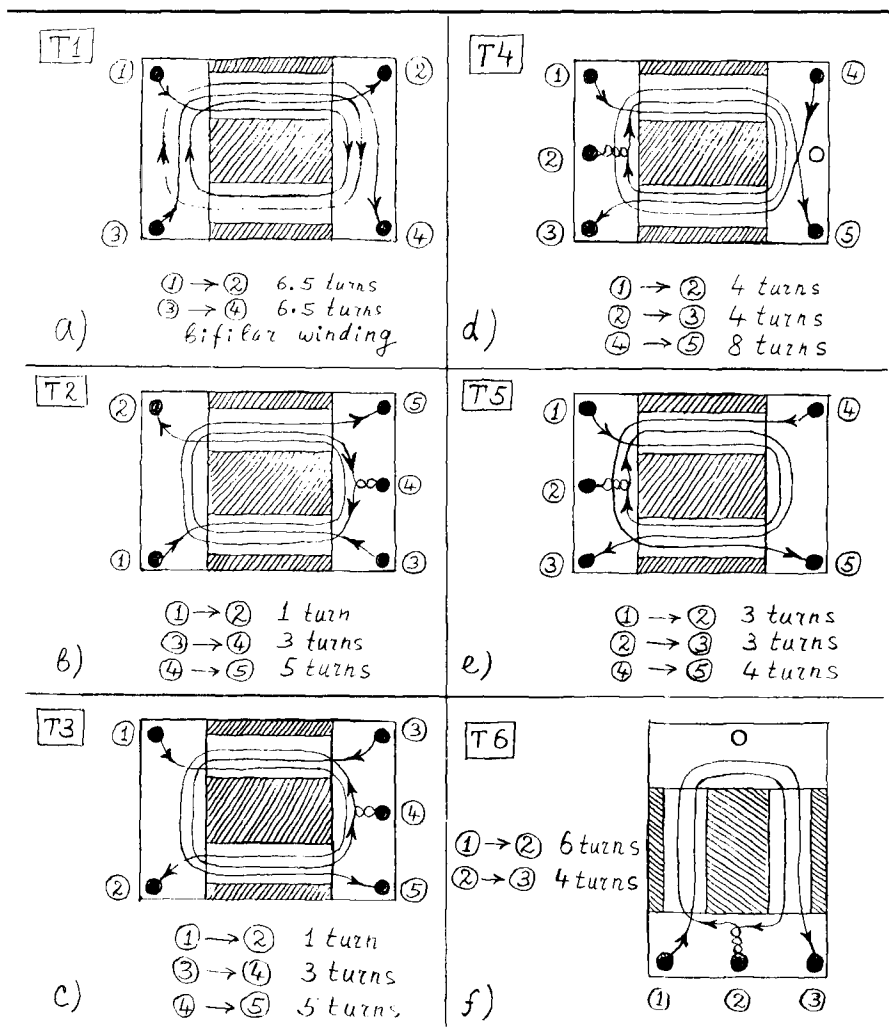


Fig 2—Transformer winding data.

5 GHz. Keeping component leads short is *essential* in order to avoid parasitic oscillations. A prerequisite for meeting the performance objectives is a high degree of symmetry between the upper and lower portions of the layout during the component mounting and transformer winding.

After the PCB drilling and counter-sinking is completed, the RF transformers and inductors L1 and L2 should be built. The transformers are built using ferrite balun cores that are mounted on top of plastic 0.3-inch-wide DIP headers. Cut off six 6-pin headers using cutters. File off excess plastic material around the perimeter to bring the header size to 0.3 by 0.4 inch. Next, bend the top portion of the pins outward 45° to facilitate the mounting of the ferrite core. All transformers are wound using #32 enameled wire. The winding data and diagrams are presented in Fig 2. The following guidelines should be used for building the transformers.

a) T1—remove the two middle pins from the 6-pin header. Wind the transformer using bifilar winding according to the diagram in Fig 2a. Mount the ferrite core vertically (on the long side) on the header to preserve symmetry, and solder the leads to the header pins. Use minimum heat to avoid melting the plastic header. Do not leave slack in the windings, and keep leads as short as practically possible. Use a small amount of adhesive to keep the core in place.

b) and c) T2 and T3—remove the middle pin from the primary side of the 6-pin header. Cut off the bottom portion of pins 2 and 5 on both headers; remove protruding metal with a file in order to prevent the pins from touching the ground plane. Wind T3 according to the diagram in Fig 2c. Wind the primary first and the secondary on top of it. Mount the core horizontally on the header and solder the leads. T2 is a mirror image of T3 and can be built by duplicating the T3 transformer and flipping the core before mounting it on its header (see Fig 2b).

d) T4—cut off the top portion of the middle pin on the secondary side of the header. Cut off the bottom portion of pins 4 and 5 and remove all protruding metal. Wind T4 according to the diagram in Fig 2d. Wind the primary first and the secondary on top of it. Note that the leads from the secondary cross each other for proper phasing.

e) T5—remove the middle pin from

the secondary side of the 6-pin header. Cut off the bottom portion of pins 1 and 3 and remove all protruding metal. Wind T5 according to the diagram in Fig 2e.

f) T6—remove two outside pins on the top side of the header. Cut off the top portion of the top middle pin. Wind T6 according to the diagram in Fig 2f. Use adhesive to keep the core in place.

The two inductors L1 and L2 are built by winding ten turns of #32 enameled wire through the hole of a small ferrite bead.

After the transformers and inductors have been built, the board construction can proceed in the following sequence.

1) Vector pins and resistors (except for R6 and R7). There are 10 Vector pins: +12 V, GND(2), R10(2), C19(2), IN, OUT300 and OUT50 (see the component placement diagram in Fig 3). Resistors are mounted flush to the PCB surface. If a component lead has to be grounded, a solder joint has to be made on the ground plane (in addition to the solder joint on the solder side).

2) Thru-hole capacitors (except for C11, C12, C17, C18) and inductors L1 and L2.

3) Transformers T1 through T6. Transformers T1, T5 and T6 have a grounded pin (see Fig 3). These pins should be soldered to the ground plane using a short piece of wire-wrap wire.

4) Transistors Q1 and Q2. Arrange two transistors with markings on the

top side. The long lead is the collector, the one opposite is the base and the remaining two are the emitters. Bend the base leads down 90°—these are the only leads soldered to the PCB.

For Q1, place the base at 10 o'clock, collector at 4 o'clock and emitter at 8 o'clock; cut off the emitter lead at 2 o'clock. For Q2, place the base at 8 o'clock, collector at 2 o'clock and emitter at 10 o'clock. Cut off the emitter and collector leads of both transistors to $\frac{3}{16}$ inch and bend the leads upward slightly. Prior to soldering the transistors into their position on the PCB, form the leads in such a fashion that they touch the two pins on the transformer header while the transistor case rests flat against the PCB surface. Trim the leads further, leaving enough length to make a reliable connection to the RF transformer. Solder the pins into position, making sure that there is no gap between the transistor case and the PCB; the copper surface provides some heat-sinking.

5) Transistors Q3 and Q4 are placed in the same fashion. Trim the collector leads of both transistors to $\frac{3}{16}$ inch and form them so they touch the two pins on the primary side of the T5 transformer header. Leave as little lead length as possible prior to soldering. Trim the emitter leads of both transistors to $\frac{3}{32}$ inch and bend them upward slightly until they align in height with the two pins on the

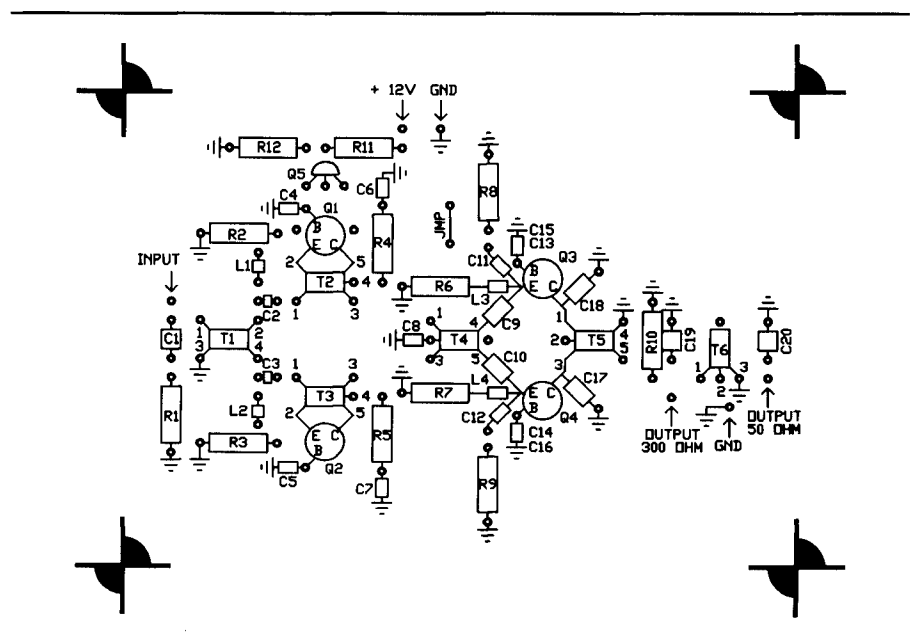


Fig 3—Component placement diagram. (Scale 1:1)

secondary side of the T4 transformer header. Solder Q3 and Q4 in place while keeping their plastic cases resting against the PCB surface. Place and solder 0.1- μ F SMD capacitors (C9 and C10) across the gap between the emitter leads and the T4 transformer pins. Apply as little heat as possible during soldering to avoid overheating the transistors and melting the plastic DIP headers.

6) Capacitors C17 and C18. The "hot" lead of trimmer capacitor C17 is soldered to the collector lead of Q4; form the leads so the capacitor base lies flat against the PCB surface. The ground lead of C17 is soldered to the ground plane at the location marked with a hole in the PCB.

7) 0.1- μ F SMD capacitors C4, C5, C6, C7, C15, C16. The "hot" lead of the capacitors is soldered directly to the component lead while the capacitor rests against the PCB surface. Make sure that the "hot" pad of the capacitor does not touch the ground plane. SMD capacitors C13 and C14 are mounted on top of C15 and C16. Capacitor C8 is mounted at an angle and soldered directly to the pin on the transformer header (tap of T4 primary).

8) SMD inductors L3 and L4 are placed flat on the PCB (with their pads up) parallel to the T4 transformer header and $\frac{1}{16}$ inch away from it. Lean the inductor against the emitter lead and solder the inductor corner to it.

9) R6 and R7. Solder these to the inductor pad on one side and to the ground plane on the other side. Holes in the PCB are provided for placement guidance. Keep resistor lead length to a minimum.

10) Capacitors C11 and C12. Form the capacitor leads so one lead can be soldered to the SMD inductor pad and the other lead can be inserted into the PCB hole connecting it to resistors R8 and R9.

11) Transistor Q5. Form the transistor leads and bend them 90° so the flat side of the TO-92 case rests flush against the case of Q1. Prior to soldering Q5 in place, apply a small amount of silicon thermal compound between the two surfaces. To further improve the thermal coupling, form a loop out of hook-up wire and place it over the TO-92 case. Feed the ends of the loop into holes provided in the PCB; tighten the loop prior to soldering it in place.

12) Q3 and Q4 heat sinks. These serve the dual purpose of heat sinking and shielding. Form two heat sinks out of 0.015 to 0.020-inch sheet metal (tinned steel, brass or copper) accord-

ing to the drawing in Fig 4. Place the heat sinks over transistors Q3 and Q4, making sure that the metal strips rest flush against the transistor cases, and solder the bottom portions of the heat sinks to the ground plane symmetrically.

13) Install a jumper made of insulated wire above resistor R6.

14) Prepare two short (less than 3 inches) coaxial cables with a BNC connector on one end and a solder tail on the other end. Solder the center conductors to the input and output Vector pins and the outer shield to the ground plane.

Alignment

Before alignment can proceed, the dc bias has to be verified. The bias voltage (VB) applied to all four transistor bases has to be 2 V. If it deviates more than $\pm 5\%$ from the nominal value, adjust the value of R12. The dc voltage on the emitters of Q1 through Q4 should be $1.27 \text{ V} \pm 5\%$.

I assumed that the resistance of the SMD inductors L3 and L4 is 4.5 Ω . If not, adjust the values of R6 and R7 for a combined series resistance of 25.5 Ω .

If the directions are followed while building the RF transformers, the network C1-R1 should require no adjustment. The value of resistor R10 is selected to establish a 300- Ω output impedance. Impedance values other than 300 Ω are obtained by implementing the modifications listed in Table 1. R10 values in Table 1 are calculated values; actual output impedance may differ slightly. The

required value may be easily obtained by temporarily substituting R10 with a 2-k Ω potentiometer and adjusting its value until the desired output impedance is obtained.

The values of capacitors C19 and C20 may have to be changed if a change in T5 and T6 transformation ratios is called for by Table 1. The required values may be determined by using a variable capacitor and peaking the output signal at the IF frequency. A low-capacitance (FET) probe is recommended for this procedure. If a 1:10 scope probe is used, its capacitance (typically 10 to 13 pF) should be subtracted from the obtained capacitance value.

Adjusting trimmer capacitor C17 for the minimum level of the IMD products should be the last step of the alignment procedure. A five-minute

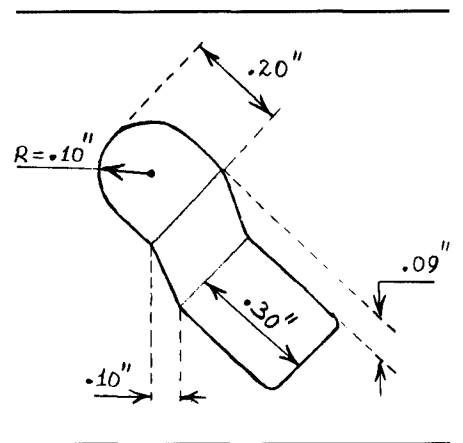


Fig 4—Q3 and Q4 heat sinks.

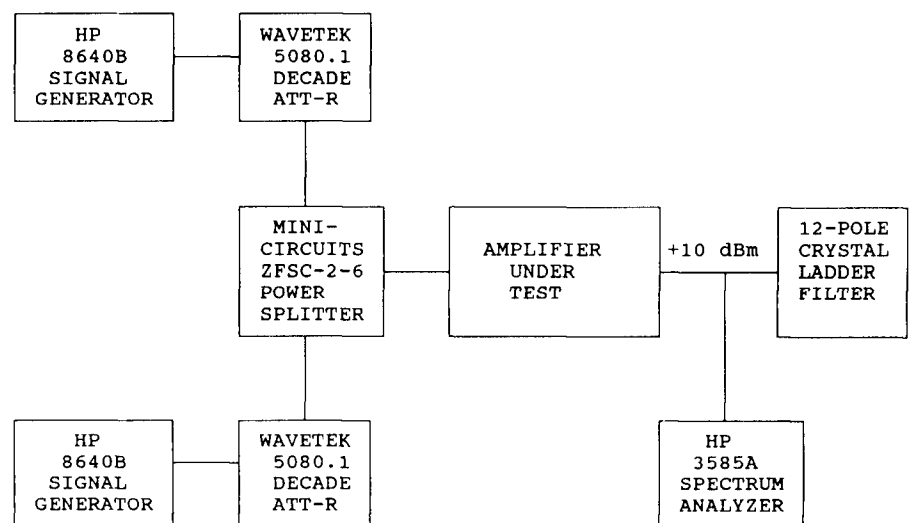


Fig 5—Alignment/measurement setup.

warm-up time has to be given to allow the TIA to reach its nominal temperature. A two-tone source is required to perform this adjustment. A block diagram of the IMD alignment and measurement setup is given in Fig 5. During the alignment procedure, the crystal filter is removed and replaced with the 50-Ω input impedance of the spectrum analyzer. This adjustment procedure can also be successfully performed using home-built equipment. An example of a two-tone signal source including a 6-dB hybrid combiner is given in Note 6.

If a spectrum analyzer is not available, an alternate method can be used. It requires a receiver with an 8 to 9-MHz IF strip. Connect the TIA to the input of the IF strip; make sure the TIA output is properly terminated. Disable the AGC. Monitor the signal at the output of the IF strip with an oscilloscope. Apply the two-tone signal source to the input of the TIA. Adjust the frequencies of the two signal sources so one of their third-order products ($2f_1 - f_2$ or $2f_2 - f_1$) falls into the passband of the IF strip. Adjust the amplitudes of the signal sources so the level of the product at the IF strip output is at least 20 dB above the noise level. The frequency separation between the two tones can be between 20 and 100 kHz. Adjust the trimmer capacitor C17 for the lowest level of the IMD product; use a plastic adjustment tool.

This method requires the use of two variable-frequency signal sources. It is also possible to use a two-tone signal from two crystal-controlled sources. The combined signal can be injected at the antenna terminals or at the input of the mixer. The VFO is then tuned to place the third-order product in the IF passband. There is a drawback with this method: stages preceding the TIA may cause IM distortion and mask the IMD products developed in the TIA, making the adjustment impossible.

Measurements

After the TIA alignment was completed, a set of measurements was performed using laboratory-grade measurement equipment.

Fig 6 shows the TIA input impedance from 1 MHz to 100 MHz measured with an HP4194A impedance analyzer. Fig 7 and Fig 8 show the TIA output impedance at the 300-Ω and 50-Ω nodes respectively. The measured TIA power gain is 9.5 dB.

A spectral noise-density measure-

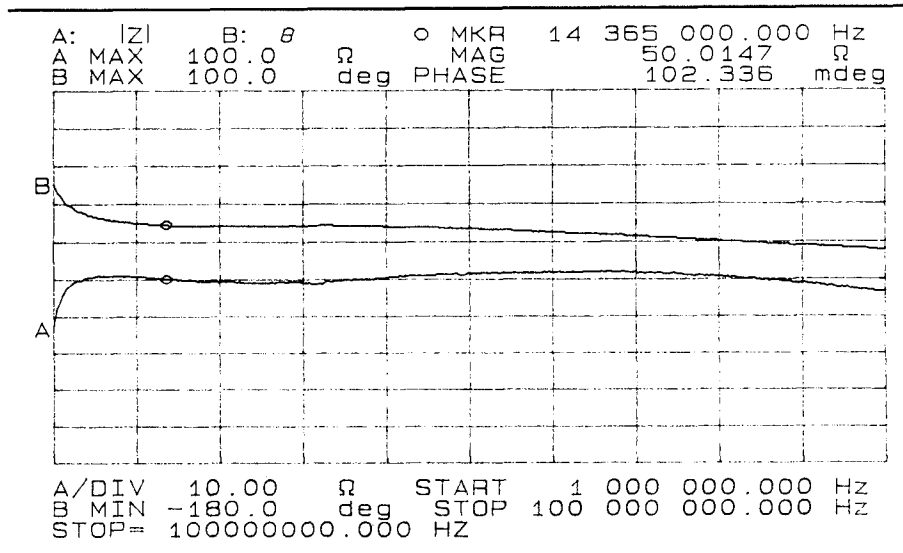


Fig 6—TIA input impedance.

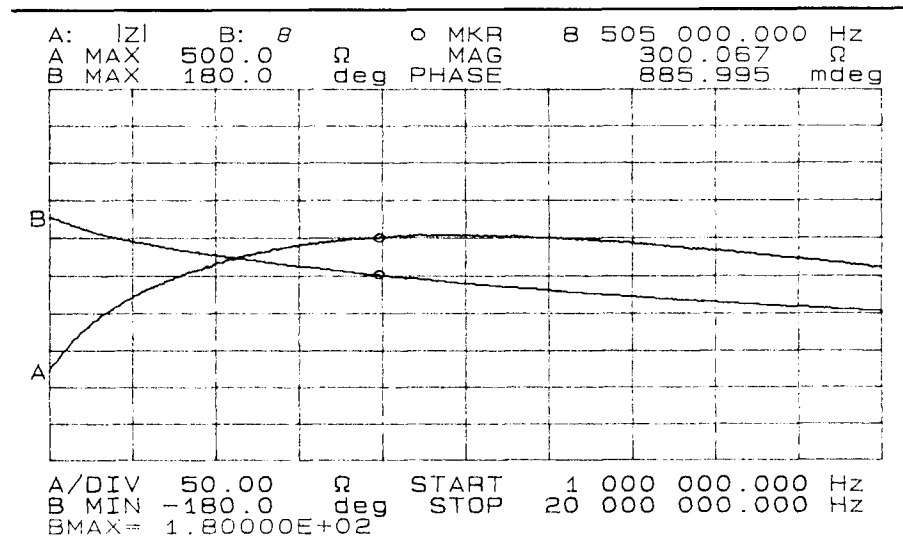


Fig 7—TIA output impedance—300 Ω.

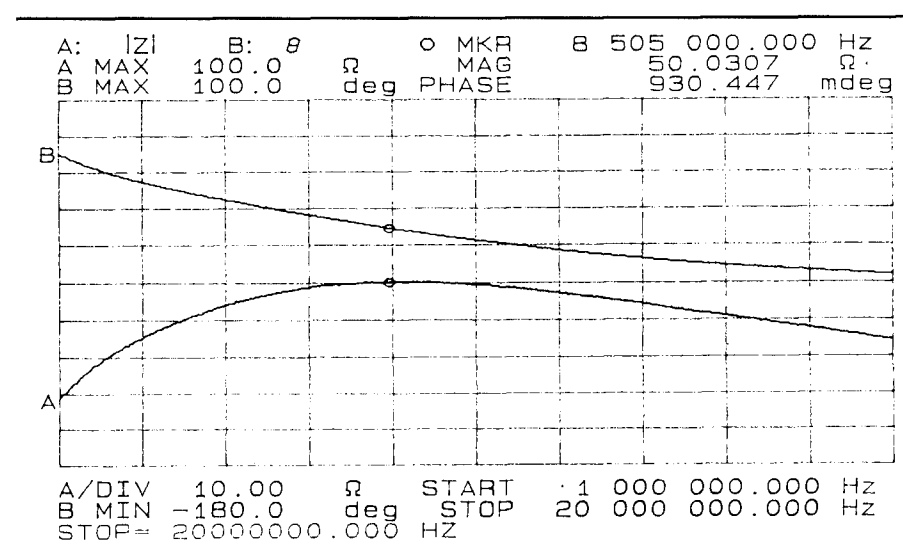


Fig 8—TIA output impedance—50 Ω.

ment at 8 MHz using the HP3585A spectrum analyzer yields a noise figure of 3.5 dB. A slight improvement can be obtained by replacing Q1 and Q2 with MRF581A transistors.

The remaining portion of the measurement was performed using the test setup in Fig 5.

The crystal filter was disconnected and the amplifier was loaded with the 50- Ω input impedance of the analyzer. The frequencies of both generators were set to around 8 MHz, and frequency separation was kept at 20 kHz throughout the measurements.

The 1-dB desensitization point (or 1-dB compression point due to blocking) was measured by setting the level of one of the signal sources 50 dB below the level of the other source. The level of the stronger signal was increased to a point where the amplitude of the smaller signal decreased by 1 dB. The 1-dB desensitization point at the TIA output was found to be equal to +23.5 dBm. The 1-dB desensitization point at the input is +14 dBm.

The 1-dB compression point was measured by disabling one generator, increasing the signal level from the second generator and noting the point when the signal level at the TIA output deviated from linear response by 1 dB. The 1-dB compression point at the TIA output was found to be equal to +25.5 dBm. The 1-dB compression point at the input is +16 dBm.

In order to measure the IP_{3out} , two equal-amplitude tones were adjusted to produce +10 dBm signals at the output of the TIA (see Fig 5). With C17 adjusted for a minimum level of IMD, the third-order products were measured below -72 dBm (see Fig 9). Calculation of IP_{3out} yields +51 dBm (into a resistive load). IP_{3in} at the TIA input is +41.5 dBm.

In the last measurement a 12-pole crystal ladder filter ($f_0 = 8$ MHz, BW = 2.5 kHz, $Z_{in} = 50 \Omega$) was connected to the output of the TIA. The 1-M Ω input of the spectrum analyzer was used during this test. The TIA was evaluated for its IP_{3out} performance, and it was compared with that of a BLFA biased at 45 mA.

Since it was found that the level of the IMD products is a function of the positioning of the two-tone signal relative to the passband of the filter, measurements were performed with both tones outside of passband, one tone inside the passband and one tone at the edge of passband (see Note 2). The measurement results are summarized in Table 2. The edge of the

passband clearly presents the most difficult case, since at one edge the filter impedance abruptly drops to a value around 5 Ω while at the other edge it rises to several hundred ohms.

It has to be noted that the degradation in the IP_{3out} values occurs in the first pole or in the first few poles of the crystal filter and is reflected back to the output of the driving stage.

A 3-dB pad improves the IP_{3out} for both types of amplifiers by presenting a termination with less severe impedance variations to the driving amplifier. While the pad also has a favorable effect on the input impedance of the BLFA, it has no effect on the input impedance of the TIA. Since a 3-dB pad has only a slight effect on the overall noise figure it is a worthwhile addition.

It should also be noted that the broadband 50- Ω input impedance of the TIA eliminates the need for a diplexer as a means of presenting a broadband 50- Ω termination to the IF port of the mixer. However, the other function of the diplexer—limiting the spectrum of frequencies at the IF port of the mixer—is quite desirable. Therefore, I recommend use of the diplexer in front of the TIA; it will extend even further the frequency range of the 50- Ω resistive input impedance of the TIA and present an almost ideal termination to the mixer.

Summary

The objective of this article was to present a way to improve the intermodulation characteristics of a receiver front end by employing a

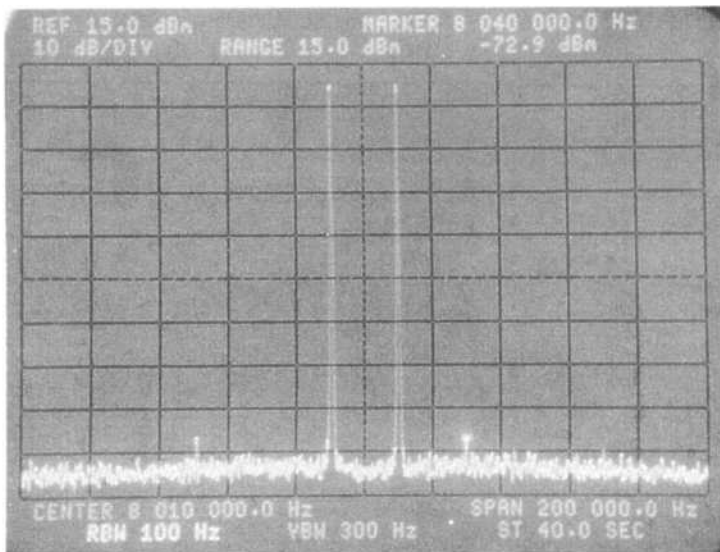


Fig 9—
IMD products
at the TIA
output—
resistive load.

Table 2— IP_{3out} measurement results.

THIRD-ORDER INTERCEPT POINT AT THE OUTPUT OF THE AMPLIFIER (+dBm)				
TONE LOCATION RELATIVE TO THE PASSBAND	BLFA		TIA	
	NO PAD	3-dB PAD	NO PAD	3-dB PAD
BOTH TONES OUTSIDE OF PASSBAND	44	45	46	48
ONE TONE INSIDE OF PASSBAND	43	46	46	47
ONE TONE AT THE EDGE OF PASSBAND	35	44	35	45

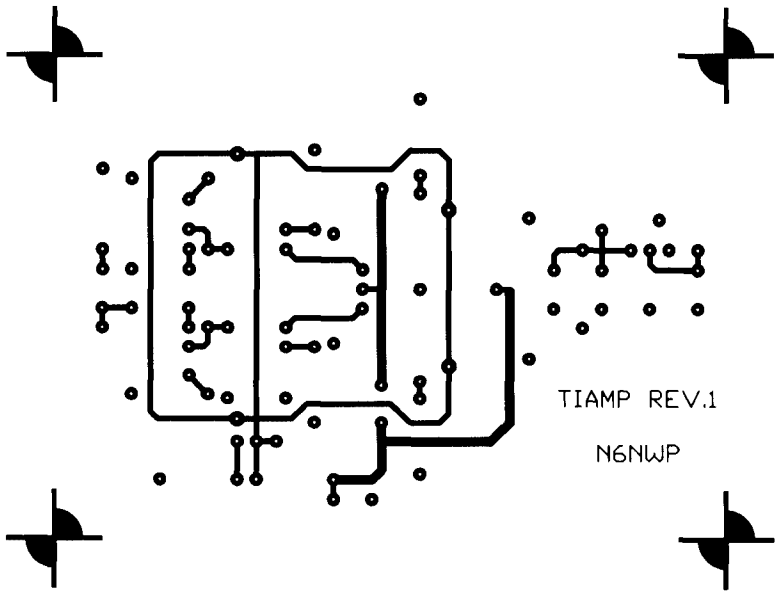


Fig 10—Solder-side layer. (Scale 1:1)

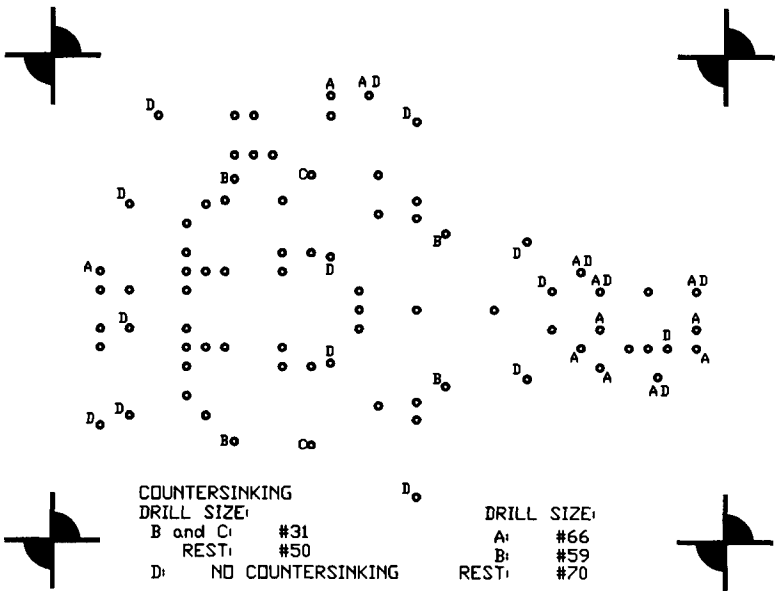


Fig 11—Component side (ground plane) drill and countersinking chart. (Scale 1:1)

“Termination Insensitive Amplifier” between the mixer and the crystal filter. This new two-stage approach allows the implementation of a flexible output circuit to match the input impedance of the crystal filter, while at the same time providing a broadband 50-Ω resistive input immune to the extreme impedance variations at the input of the crystal filter.

Such a broadband resistive termination ensures that the stages preceding the TIA experience no degradation in IMD performance due to a reactive load and allows the crystal filter to become the limiting factor in determining the IMD performance of the front end.

Due to its good linearity characteristics, the TIA makes it unnecessary to employ either fixed or electronically controlled front-end attenuators, thus simplifying the design.

Coupled with a commutation type mixer and a high-performance crystal ladder filter, the TIA may serve as a valuable building block in a high dynamic range MF/HF receiver (see Notes 2 and 3).

Notes

- ¹Norton, D., “High Dynamic Range Transistor Amplifiers using Lossless Feedback,” *Microwave Journal*, May 1976, p 53.
- ²Makhinson, J., N6NWP, “Designing and Building High-Performance Crystal Ladder Filters,” *QEX*, January 1995, pp 12-17.
- ³Makhinson, J., N6NWP, “A High-Dynamic Range MF/HF Receiver Front End,” *QST*, February 1993, pp 23-28.
- ⁴Rohde, U., KA2WEU/DJ2LR, “Key Components of Modern Receiver Design—Part 2,” *QST*, June 1994, pp 27-28.
- ⁵Horrabin, C., G3SBI, and Chadwick, P., G3RZP, “Crystal Filters for High-Performance Mixers,” Pat Hawker’s Technical Topics, *Radio Communication*, January 1994, pp 37-38.
- ⁶Hayward, W., W7ZOI, and DeMaw, D., W1FB, *Solid State Design for the Radio Amateur*, ARRL, Newington, 1986, Chapter 7: Test Equipment and Accessories.

Parts List

Designator	Part Description	Supplier
Q1-Q4	MRP581	1,2
Q5	2N4401	1,2
L1,L2	see text; core: p/n FB-43-101	3
T1-T6	see text; core: p/n BN-43-2402	3
L3,L4	33- μ H SMD inductor, size 1210; p/n DN10333CT-ND	4
R1-R12	resistor, metal film, 0.25 W, 1 $\frac{1}{2}$	1,2,4,5
C4- C10,C15,C16	0.1- μ F SMD capacitor, size 1206	2,4,5
C13,C14	100-pF SMD capacitor, size 1206	2,4,5
C17	0.3 to 3.0-pF ceramic trimmer capacitor; p/n 50F3937	1
C18	1-pF capacitor, NPO ceramic disc	2,5
C1,C11,C12, C20	100-pF capacitor, monolithic, ceramic, 0.1 to 0.2-inch lead spacing	2,4
C19	10-pF capacitor, monolithic, ceramic, 0.1 to 0.2-inch lead spacing	2,4
C2,C3	0.1- μ F capacitor, monolithic, ceramic, .1-inch lead spacing	2,4
DIP headers	0.300-inch DIP component header, low profile	1,2,3,4, 5
Vector pins	T44 miniwrap terminal; p/n V1071-ND	4

1. Newark Electronics, 312-784-5100—ask for a branch office telephone number.
2. Allied Electronics, 1-800-433-5700.
3. Amidon Associates, 310-763-5770.
4. Digi-Key Corporation, 1-800-344-4539.
5. Mouser Electronics, 1-800-346-6873.

Upcoming Technical Conferences

Eastern VHF/UHF Society Conference

August 25-27, 1995, Quality Inn & Conference Center, 51 Hartford Turnpike, Vernon, CT 06066.

Contact: San Hilinski, KA1ZE, Chairman, Pilgrim Drive, Tolland, CT 06084, tel: (W) (203) 649-3258, (H) (203) 872-6197; Ron Klimas, WZ1V (address below) or Rae Bristol, K1LXD (address below).

Events: Friday, check-in and hospitably room activities; Saturday, registration, formal talks and bandsessions; Saturday evening, banquet; Sunday, VHF-SHF Swap Meet and antenna measuring.

Registration: Registration at the door will be \$25. Preconference registration, before August 20, is \$20. Sunday-only registration is \$5. Registration fees should be sent to: Rae Bristol, K1LXD, 328 Mark Drive, Coventry, CT 06238, tel: (203) 742-8650

Reservations: The Quality Inn is offering special rates of \$51.50 per night, single or double. Call Lori Torizer at 1-800-235-4667. Be sure to mention the Eastern VHF/UHF Society to receive the special rate.

Other activities: A shopping center, \$2 movie theater and amusement area are on site.

1995 ARRL Digital Communications Conference

September 8-10, 1995, La Quinta Conference Center, Arlington, TX—just minutes from Dallas/Fort Worth Airport. Co-hosted by Tucson Amateur Packet Radio (TAPR) and the Texas Packet Radio Society.

For more information contact the TAPR office at 8987-309 E. Tanque Verde Road #337, Tucson, AZ 85749-9399, tel: (817) 383-0000; fax: (817) 566-2544; Internet: tapr@tapr.org

The 1995 AMSAT Annual Meeting and Space Symposium

October 6-8, 1995, in Orlando Florida. For more information contact: Bob Walker, 6601 SW 16th Street, Plantation, FL 33317, (305) 792-7015, email: n4cu@amsat.org.

Call for papers: The deadline for camera-ready copy is August 12. Inquiries should be sent to Bob Walker at the above address.

Microwave Update 95

October 26-28, La Quinta Inn, Arlington, TX.

For more information contact: Al Ward, WB5LUA, 2306 Forest Grove Estates Road, Allen, TX 75002 or Kent Britain, WA5VJB, 1626 Vineyard, Grand Prairie, TX 75052-1405.

Feedback

Tim Duffy, K3LR, just called my attention to the fact that I should have included the following reference in my June 1995 *QEX* article, "Torque Capacity of Keyed Rotator Shafts." It has to do with the choice of key size and material in keyed shafts. The basic issue of this paper is that the key must be at least as strong as the shaft or all the wonderful shaft material is wasted.—D. B. Leeson, W6QHS
Calistrat, M. M., "Shaft Keys Revisited," *Power Transmission Design*, May 1995, p 105. Penton Publishing, Inc, Cleveland, OH.